International Journal of Pharmaceutics 561 (2019) 47–65

Contents lists available at ScienceDirect

International Journal of Pharmaceutics

journal homepage: www.elsevier.com/locate/ijpharm

Review

How to characterize a nasal product. The state of the art of *in vitro* and *ex vivo* specific methods

Laurent Salade*, Nathalie Wauthoz, Jonathan Goole, Karim Amighi

Laboratoire de Pharmacie Galénique et de Biopharmacie, Université libre de Bruxelles (ULB), Brussels, Belgium

ARTICLE INFO

Keywords:
Nasal delivery
Characterization method
In vitro
Ex vivo
Formulation development

ABSTRACT

Nasal delivery offers many benefits over other conventional routes of delivery (e.g. oral or intravenous administration). Benefits include, among others, a fast onset of action, non-invasiveness and direct access to the central nervous system. The nasal cavity is not only limited to local application (e.g. rhinosinusitis) but can also provide direct access to other sites in the body (e.g. the central nervous system or systemic circulation). However, both the anatomy and the physiology of the nose impose their own limitations, such as a small volume for delivery or rapid mucociliary clearance. To meet nasal-specific criteria, the formulator has to complete a plethora of tests, *in vitro* and *ex vivo*, to assess the efficacy and tolerance of a new drug-delivery system. Moreover, depending on the desired therapeutic effect, the delivery of the drug should target a specific pathway that could potentially be achieved through a modified release of this drug. Therefore, this review focuses on specific techniques that should be performed when a nasal formulation is developed. The review covers both the tests recommended by regulatory agencies (e.g. the Food and Drug Administration) and other complementary experiments frequently performed in the field.

1. Introduction

For many years, nasal administration has been limited to the local delivery of vasoconstrictors or anti-inflammatories (Pires et al., 2009). Subsequently, the potential of nasal administration for systemic delivery, mucosal vaccination and nose-to-brain delivery has been considered. First, the systemic delivery of drugs was envisaged due to the dense vascularization of the nasal mucosa. This pathway appeared to be an attractive alternative to conventional administration, in particular for drugs inactivated by the oral route (Türker et al., 2004). Many examples of nasal administration with systemic diffusion (e.g. morphine (Stoker et al., 2008; Pavis et al., 2002) or metoprolol (Kilian and Müller, 1998) have already been cited in the literature, including the use of biotherapeutics (e.g. insulin (Varshosaz et al., 2006). Some of them are marketed, such as Miacalcin® (Novartis, East Hanover, USA) or Minirin® (Ferring Pharmaceuticals, Saint-Prex, Switzerland), which contain salmon calcitonin and desmopressin, respectively. The nasal cavity has also been considered as a potential immunization site for vaccine administration as it is the first site of the body to be exposed to inhaled antigens (Csaba et al., 2009; Davis, 2001). For instance, both preclinical and clinical studies have already emphasized satisfactory immune responses following the nasal administration of inactivated influenza vaccine (Terauchi et al., 2018; Dehghan et al., 2018). The influenza vaccines Flumist® (brand name Fluenz Tetra in Europe) from AstraZeneca (Cambridge, UK) and Nasovac® from Serum Institute of India (Pune, India) have been approved in the USA and India, in 2003 and 2010 respectively (Bahamondez-Canas and Cui, 2018). More recently, nasal administration has been proposed to deliver drugs directly to the central nervous system (i.e. nose-to-brain delivery) while avoiding the blood-brain barrier (BBB) (Illum, 2004). Indeed, the BBB is known to be the major obstacle to brain access for xenobiotics. Therefore, nose-to-brain delivery offers a great opportunity to deliver both conventional chemical drug and biotherapeutics for the treatment of brain diseases such as neurodegenerative pathologies (e.g. Alzheimer's or Parkinson's disease) (Sekerdag, 2017) or brain cancers (e.g. glioblastoma) (van Woensel et al., 2013), while avoiding the use of invasive techniques to reach the brain (Kumar et al., 2018).

However, when such potent drugs or biopharmaceutics are administered nasally, issues may appear due to their physicochemical properties (i.e. solubility, molecular weight and stability) (Wen, 2011).

Abbreviations: ALI, Air Liquid Interface; BBB, Blood Brain Barrier; BEG, Bronchial Epithelial Cell Growth Medium; LLC, Liquid Covered Culture; NGI, Next Generation Impactor; P_{app}, Apparent Permeability Coefficient; PBS, Phosphate Buffered Saline; PLGA, Poly(lactic-*co*-glycolic acid); PSD, Particle Size Distribution; PTFE, Polytetrafluoroethylene; TEER, Transepithelial Electrical Resistance

* Corresponding author.
E-mail address: lsalade@ulb.ac.be (L. Salade).

https://doi.org/10.1016/j.ijpharm.2019.02.026
Received 9 January 2019; Received in revised form 15 February 2019; Accepted 15 February 2019
Available online 26 February 2019
0378-5173/

Additional troubles related to the anatomical specificity of the nasal cavity can also be encountered during administration (e.g. rapid elimination of the formulation by the mucociliary clearance). To overcome such limitations, effective pharmaceutical formulations need to be developed. The formulation strategies can combine nanotechnologies and excipients acting on nasal residence in order to fight against the mucociliary clearance (e.g. thickening or mucoadhesive excipients) on the permeability through the epithelial barrier (when a systemic or nose-to-brain transfer is considered) or on the drug protection against enzymatic digestion (when sensitive drugs such as peptide are administered) (van Woensel et al., 2013).

A few reviews have addressed in detail the formulation aspect of nasal administration, with a special focus on: nanocarriers for nose-to-brain delivery (Sonvico et al., 2018), nasal powders (Tiozzo Fasiolo et al., 2018), mucoadhesive polymers (Chaturvedi et al., 2011), nasal formulation parameters (Dondeti et al., 1996), chitosan for nasal formulations (Casettari and Illum, 2014) and the nasal delivery of high molecular weight drugs (Ozsoy et al., 2009). Besides the formulation aspect, nasal delivery requires a device to aerosolize the formulation to allow its deposition in the nasal cavity. For instance, depending on the physical state of the formulation (e.g. powder or liquid) or the specific therapeutic scheme (e.g. chronic vs. single administration), the device is selected from: single- or multiple-dose devices; liquid, semi-solid or powdered formulation devices; pressurized or unpressurized devices (Djupesland, 2013). Moreover, some devices can specifically target the olfactory mucosa (in the case of nose-to-brain delivery) whereas others can deliver very accurate doses while avoiding losses in the deeper respiratory tract (Djupesland, 2013; Luthringer et al., 2009).

The formulation, including its excipients as well as the formulation-device combination (i.e. the generated aerosol), need to be characterized to justify both excipient and device choice and to evaluate tolerance of the formulation (Ument Karasulu et al., 2008). For such purposes, *in vitro* and/or *ex vivo* experiments can be performed before proceeding to *in vivo* preclinical and clinical evaluations. Consequently, the aim of this review is to set out the *ex vivo* and *in vitro* tests recommended by regulatory agencies and the complementary tests specific to the nasal field. *In vivo* methods were not addressed in this manuscript in order to focus on other categories of techniques (*in vitro* and *ex vivo*) and thus provide more detailed information to the reader.

2. Nasal anatomy

The nasal cavity begins at the entrance of the nostrils where the vestibule is located (Fig. 1) (Harkema et al., 2006). Posteriorly to the vestibule, there is the main chamber covered by the “respiratory mucosa” where protuberances named “turbinates” are apparent with inferior, middle and superior turbinates. In the upper part of the nose is found the “the olfactory mucosa”. The nose is separated into a couple of sections by a partition called the “nasal septum”. The nasal cavity is characterized by a surface of 180 cm^2 which is due to the presence of microvilli but also to the presence of the turbinates. The different parts of the nasal cavity are covered by 4 distinct types of epithelium (Harkema et al., 2006):

(1) The squamous epithelium essentially represented in the vestibule
(2) A ciliated pseudostratified cuboidal epithelium (also called respiratory mucosa) that lies on the most part of the nasal cavity
(3) The transitional epithelium that is a cuboidal non-ciliated epithelium located in a narrow zone that makes the transition between the squamous epithelium and the respiratory mucosa
(4) The olfactory epithelium (also called the olfactory mucosa)

The nose has a total volume of 15 mL, a length of 12–14 cm and presents a pH range of 5.5–6.5 (Gizurarson, 1993; England et al., 1999). The temperature in the nose is slightly below the human body temperature and ranges between 33 and 35 °C (Foxman et al., 2015).

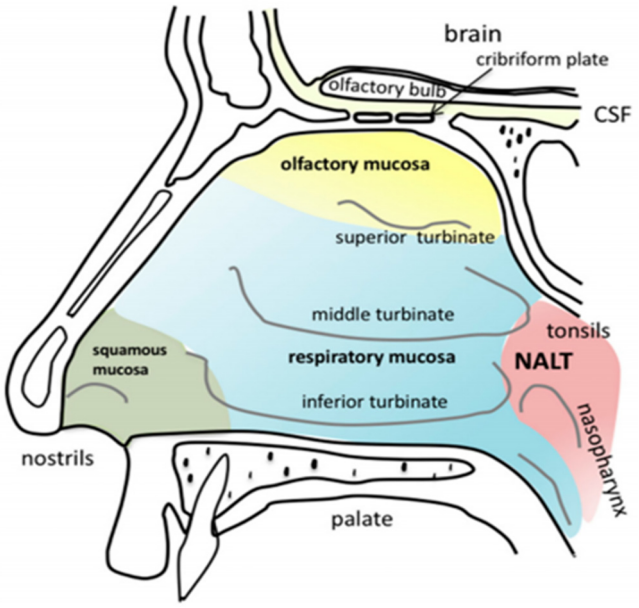

Fig. 1. Anatomy of the human nasal cavity (NALT: Nasopharynx-associated lymphatic tissue) (reproduced with authorization) (Gänger and Schindowski, 2018).

Thanks to its respective mucosa, the nose allow a molecule to be transferred to other anatomical sites. Indeed, due to its high vascularization, the respiratory mucosa can provide a good site for the transfer of drugs from the nose to the systemic circulation (Illum, 1996). On the other hand, the olfactory mucosa may provide a direct transfer of a drug from the nose to the brain while circumventing the BBB. Indeed, this is the only place in the body where the central nervous system is directly connected to the external environment, thanks to the olfactory nerves (Pardeshi and Belgamwar, 2013).

In addition to other tasks attributed to the nasal cavity (i.e. olfaction and respiration), the nose is one of the first defence barriers against external toxins and microbes.

It is therefore equipped with a rapid mucociliary clearance, in which the mucus is displaced at a rate of 5 mm/min, with a turnover of 15–20 min (D'Souza, 2015). This justifies the use of mucoadhesive agents to increase the drug residence time in the nose. The barrier function is also ensured by the presence of multiple nasal enzymes, macrophages, humoral mechanisms, etc (Beule, 2010). Another anatomic relevant parameter of the nasal mucosa is the presence of tight junctions that limit permeability through the mucosa (Lin et al., 2016). These effective defence mechanisms result in a rapid elimination and poor permeability of deposited particles. Therefore, effective formulation strategies have to be developed to overcome such limitations.

3. Physico-chemical characterization of nasal formulations

3.1. Liquid formulations

Usually, nasal liquid formulations are either aqueous simple solutions, micro- or nano- suspensions or emulsions (Djupesland, 2013). The volume usually delivered in the nose is in the range 25–150 µL, with an upper limit of 200 µL (Bhise et al., 2008). The nasal cavity may support a wide range of osmotic pressures before being altered (e.g. epithelium damage, increased mucus secretion), but it should ideally be close to ~280 mOsmol/Kg (Gibaldi et al., 2007). However, some nasal marketed products have reported an osmolality in the range 300–600 mOsmol/Kg. The formulation pH may interfere with the natural function of nasal lysozymes, which are defence enzymes active under acidic conditions36, (Shinichiro et al., 1981; Ellison and Giehl,

1991). It may also affect the solubility and permeation of a drug presenting (an) ionizable group(s) and/or may have an effect on its stability (Huang et al., 1985). To respect the physiology of the nose, the ideal pH of a nasal formulation should be between 4.5 and 6.5. Moreover, the rheological properties of the formulation should be assessed, especially when its viscosity could change once delivered to the nose (e.g. *in situ* gelling systems) (Cai et al., 2011). Viscous formulation may be desired as they are associated with prolonged retention time and slower flow through the nasal cavity. However, nasal obstruction during administration can occur and the formulation spreadability can be diminished. In addition, viscosity has a direct impact on the aerosol droplet size distribution. Therefore, it directly influences the drug distribution in the nasal cavity.

Moreover, when formulations are dispersed systems (e.g. micro- or nano- suspensions or emulsions), size and charge evaluations are usually performed by laser diffraction or dynamic light scattering and electrophoretic mobility, respectively (Salade et al., 2017). Transmission electron microscopy is another qualitative tool, which provides information about the size, shape and surface aspect of colloids (Pathak and Thassu, 2009).

3.2. Powder formulations

Depending on the powder density, a maximum of 50 mg is usually considered as acceptable for the delivery of a nasal-powdered formulation (Gad and Wiley InterScience, 2008). The flow properties may be evaluated by different methods (e.g. angle of repose, compressibility index or Hausner index, flow rate through an orifice, shear cell), as described in the European Pharmacopoeia, 7th Edition, section 2.9.34. The residual moisture of the formulation can be estimated by weight evaluation before and after desiccation, by thermogravimetric analysis or by accurately determining the water content using a Karl Fisher test. The residual moisture in the formulation is an important parameter for powder properties as well as for drug stability (Salade et al., 2018). The flowability of the powder may be improved by the presence of small amounts of residual moisture as water can act as a lubricant by reducing electrostatic charges. However, excess water can cause the formation of liquid bridges and thus limit the correct dispersion of the powder during aerosolization (Crouter and Briens, 2014). For example, during the development of a spray-dried influenza vaccine with potential lung or nasal application, a maximum limit of 3% residual moisture was established (Kanojia et al., 2016).

4. Evaluation of formulation behavior in the nasal cavity

Once the formulation has been developed, *ex vivo* and *in vitro* tests need to be performed to evaluate biological aspects (i.e. permeation, mucoadhesion, cilia and/or cell toxicity, etc.).

4.1. Assessment of the drug permeation

Permeability studies can provide relevant data about the drug transport through an epithelium or about the effect of an excipient on drug permeability (McMartin et al., 1987). Permeation models are based on either *ex vivo* methods, using excised nasal mucosa, or *in vitro* methods based on *in vitro* cell culture models. The formulation of interest needs to be deposited homogenously and reproducibly on the excised nasal mucosa or on the apical side of the cell layer without damaging the tissue. The epithelium integrity can be controlled by determining the transepithelial electrical resistance (TEER). This is the electrical resistance between the apical and basal compartments and is calculated using the following equation (Eq. (1)) (EVOM2):

$$TEER\ (\Omega * cm^2) = Resistance\ (\Omega) x\ Effective\ membrane\ area\ (cm^2) \quad (1)$$

The TEER can be determined using different methods, including hand-held electrodes and EndOhm chambers (Foster et al., 2000). Attention must be paid to selecting the electrode model as this choice depends on the precision needed and the insert used. Hand-held electrodes have a high reading variation (5–10%) and can be used for small inserts (diameter < 24 mm). In comparison, chamber configurations can deliver a uniform density through larger membranes (diameter ≥ 24 mm), with a reduced reading variation (Srinivasan et al., 2015).

Both excised mucosa and cell layers require an equilibrium time (~30 min or 60 min (Röhm et al., 2017; Lungare et al., 2016; Wang et al., 2017; Li et al., 2006) before performing the permeation study, which then consists of taking aliquots from the basal compartment at regular intervals (Gonçalves et al., 2016). The deposition of a reproducible and uniform amount of drug on the tissue is thus crucial as it will directly influence the gradient concentration and could thus introduce variation in the permeability (Upadhyay et al., 2017).

4.1.1. Formulation deposition methods

Before carrying out the test, the formulation must be deposited on the tissue in a homogeneous and reproducible manner. Ideally, this should be done in a similar way to the intranasal administration performed in the patient: simple deposition, in the case of droplets, or aerosolization, in the case of sprays. However, during drug permeation studies, liquid formulations are usually dropped directly on the excised tissue or cell layer using micropipettes, even if the formulation is intended to be aerosolized in the patient. Moreover, a precise but relatively large volume of formulation is deposited, which does not represent the small volume (max. 200 µL per nostril) actually administered in the patient (Gad and Wiley InterScience, 2008). For powders, the deposition is made either after the extemporaneous dispersion of the powder in a liquid or by aerosolization from a device.

This aspect was addressed in an interesting work comparing the permeability of ketoprofen in five powder formulations delivered either as solutions, dispersions (i.e. a powder previously dispersed in a liquid) or “powders” (i.e. extemporaneous dispersion in a liquid just before the deposition) through RPMI 2650 cell layers (Gonçalves et al., 2016). Powder deposition showed the highest variability regarding ketoprofen permeability in comparison with the deposition of solutions and dispersions. This result was probably due to the heterogeneity of concentrations at the surface of the cell layer. This study highlighted the difficulty of depositing a powder homogeneously and the need to predisperse the powder in a liquid to reach sufficient reproducibility. However, the addition of solvent does not properly represent the behaviour of the powder once administered in the nasal cavity.

Another means of depositing powder on epithelia or cell layers is to form an aerosol. In this case, the powder deposition should not result in any damage to the epithelium or cell layer. Therefore, the deposition method needs to be selected carefully and properly evaluated. The distance separating the nozzle from the cell layer or epithelium must be adapted to the aerosol velocity of the formulation particles. The epithelium integrity can be assessed by comparing TEER values before and after deposition of an inert powder (e.g. lactose) on the cells. The deposition of a reproducible and accurate amount of drug can also be assessed on the basis of a gravimetric protocol (if the powder is homogeneous) or by quantification of the drug, after deposition.

An interesting work focused on powder deposition with an aerosol generated from the Rhinocort® nasal spray (AstraZeneca, North Ryde, NSW, Australia) (Pozzoli, 2017). To this end, the authors developed a new 3D-printed expansion chamber that retains the powder that would be deposited in the nasal cavity. The novelty is in the chamber design, which includes a location for inserts with RPMI 2650 cells. This configuration allowed study of the drug permeation from the powder once it is deposited. In this case, the amount of budesonide deposited in this new expansion chamber was 98.73 ± 0.09% of the nominal dose (n = 3). In the three inserts loaded in the chamber, 13.12 ± 0.07 µg of budesonide could be recovered. The integrity of the cell layer was also confirmed, with no significant TEER difference ($p > 0.05$) between the

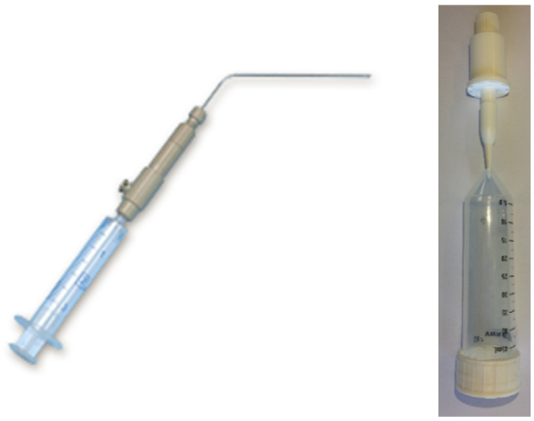

Fig. 2. Illustration of the DP-4™ insufflator from PennCentury (© PennCentury) (left) and the UDS® device from Aptar Pharma (© Aptar Pharma Group) equipped with a nozzle for rats and coupled to a Falcon® tube, where the insert was placed instead of the cap (right).

initial value (126 ± 21 Ω.cm^2) and the value after the permeation test (127 ± 14 Ω.cm^2). This model was validated this way to assess both aerosol deposition and permeation.

Another alternative is the Dry Powder Insufflator™ Model DP-4 (Fig. 2) from Penn-Century (Penn-Century Inc., Philadelphia, PA), developed for different animal models. These devices aerosolize powder contained in their reservoir through their tip using air from a syringe. They were initially intended to deliver powders into lungs of rats (DP-4R) or mice (DP-4 M) after inserting the tip into the trachea of the anaesthetized animal. However, the DP-4 device has also been used to deliver powder into the nasal cavity of rats (Giuliani et al., 2018) and to deposit powder onto Calu-3 monolayers under an air-liquid interface (ALI) (Meindl et al., 2015; Cingolani, 2017).

The influence of the deposition conditions of both liquid and powder aerosols on a Calu-3 cell layer was evaluated by Meindl et al. (2015). Different drugs were administered either using a Microsprayer IA-1C (Penn-Century Inc., Philadelphia, PA) for liquids or a DP-4 insufflator for powders by placing the tip 11 cm above the 1.12 cm^2 membrane area. The efficacy in terms of quantity delivered and reproducibility of the delivery, as well as the safety of the procedure in terms of guaranteeing the cell layer integrity were evaluated. With liquid aerosols generated from the Microsprayer IA-1C, no significant decrease in TEER (> 100 Ω.cm^2) was observed after deposition, suggesting a safe procedure. The delivery for liquid formulations was reproducible and presented low variability (27 ± 3%). On the other hand, the powder deposition with the DP-4 device led to a decrease in the TEER (> 100 Ω.cm^2) and the efficacy of delivery was subject to drug-specific variations (range 3–28%). The authors proposed to increase the distance between the tip and the cell layer to prevent any effect on the barrier integrity. Regarding the delivery efficacy, some powder formulations were retained strongly in the device (e.g. 50% for sodium fluorescein).

Another configuration for powder deposition was proposed with the Unit Dose System (UDS) device from Aptar Pharma (Le Vaudreuil, France) (Fig. 2). The UDS device was combined with the nozzle designed for nasal administration in rats (Aptar Pharma, Le Vaudreuil, France) and the system was connected to a 50 mL Falcon® tube pierced on the top. An insert with a surface area of 4.2 cm^2 was then placed below these instead of the cap (tip-cell layer distance = 12 cm). From the initial amount of powder loaded in the device (25 mg), 99.6% ± 1.5% was delivered and 64 ± 4.8% deposited on the Calu-3 cell monolayer on the insert, with a very good reproducibility (< 10%) (Salade et al., 2018). Of course, the reproducibility of the method could change according to the properties of the powder studied (e.g. density, cohesiveness). Powders with a high density and strong propensity to agglomerate can provide poor aerosolization properties (i.e. a poor delivered dose) and therefore a limited amount of powder deposited (e.g. stickiness in the sample chamber of the device) (Minne et al., 2008).

These observations highlight the complexity of administering powders in a uniform, effective and safe manner.

4.1.2. Ex-vivo models

Ex vivo models consist of extracting the whole tissue from either animal or human donors (Pandey et al., 2017). To preserve the tissue viability, the time elapsed between the animal sacrifice, the tissue excision and the permeation test should be as short as possible (e.g. 0.5–4 h) (Pund et al., 2013; Naik and Nair, 2014). For instance, the viability of bovine and rabbit nasal mucosa has been estimated at 3 and 10–12 h, respectively, (Bechgaard et al., 1992; Schmidt et al., 2000). Depending on the application intended for the tissue, precautions should be taken with regards to the tissue handling. For instance, cellular deaths were highlighted by Nicolazzo et al. after freezing (i.e. −20 °C for 1 month) buccal mucosa (Nicolazzo et al., 2003). However, the freezing step did not involve any modifications of its barrier integrity (confirmed by the non-diffusion of fluorescent dextrans) or its permeation properties (no effect on both caffeine and estradiol flux). These results suggest that the tissue can still be used for permeation tests69, (Borchardt et al., 1996).

Among the different species used as tissue donors, rabbit (Colombo et al., 2016), sheep (Naik and Nair, 2014), goat (Basu and Maity, 2012), calf and pig (Viegas et al., 2016) are described in the literature. Due to the limited stock of human nasal mucosa, studies have been conducted to compare histologically and morphologically both animal and human nasal mucosa. Sheep nasal mucosa presents a permeation similar to human nasal mucosa and can thus be used for both permeation and mucoadhesion experiments (Gardiner et al., 1996; Illum, 1996; Shaw et al., 2000). This has been supported by the correlation established for insulin permeation between sheep and humans31, (Illum et al., 1994; Longenecker et al., 1987; Nolte et al., 1990). However, if human nasal mucosa is still needed, it can be obtained from patients undergoing surgery in hospitals (e.g. for nasal obstruction) (Pandey et al., 2017).

For the tissue sampling site, different zones of the nasal cavity may be exploited. For instance, the olfactory mucosa can be easily differentiated from the pink respiratory mucosa due to its yellowish aspect caused by the presence of a coloured pigment (i.e. carotenoid) (Vasa et al., 2017; Moulton, 1971; Graziadei, 1971; Amoore et al., 1971). Additional protocol steps have been proposed after tissue collection, such as the step of delipidation with organic solvents (chloroform, methanol) (Karasulu et al., 2008). The goal of such removal is to avoid any UV interferences (e.g. during the quantification step) that could come from absorbance by the lipids from the tissue. Unfortunately, the use of such solvents may involve drastic permeation changes in the tissue (Ponec, 1992; Costin et al., 2009).

Once the tissue is recovered, it is fixed on a Franz cell diffusion apparatus. It is fixed between a donor chamber, which receives the formulation, and a receptor chamber, which is filled with the receptor medium (Fig. 3). The mucosa must be oriented with the mucosal side facing the donor chamber. The thickness of the tissue (usually 200 µm) should be measured and mentioned as it is directly linked to the diffusion rate (Tas et al., 2009; Shah et al., 2015; Acharya et al., 2013). The influence of the thickness was investigated in a study that compared the permeation of both hydrophilic (i.e. caffeine) and lipophilic (i.e. estradiol) molecules though either full-thickness or epithelial tissue from buccal mucosa (Nicolazzo et al., 2003). As expected, the diffusion of both caffeine and estradiol through the epithelial tissue increased 1.8-fold and 16.7-fold, respectively, in comparison with the full-thickness tissue. This shows how the tissue thickness is a crucial parameter that directly influences the diffusion rate.

The selection of the receptor medium composition is also crucial as it can strongly influence the quality of the experiment.. It should fulfil

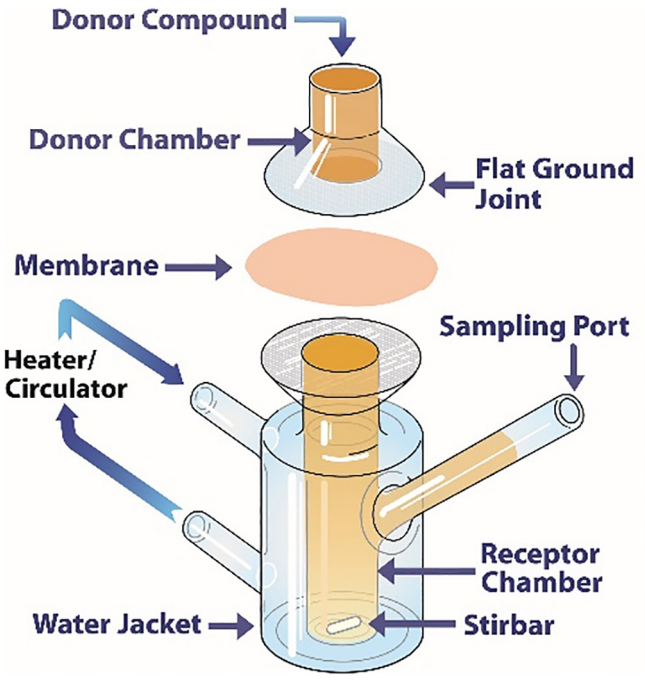

Fig. 3. Vertical Franz cell diffusion (© PermeGear) (reproduced with authorization).

"sink" conditions to avoid any influence of the drug that already diffused on the diffusion rate of the drug still remaining in the formulation (Ng et al., 2010). During the permeation test, water can circulate in a double jacket to standardize the temperature. This temperature is fixed at 37 °C in many permeation studies. However the temperature of the nasal mucosa is a bit little lower and the temperature fixed should not exceed 34.4 ± 0.1.1 °C (Lindemann et al., 2002).

In addition to its use in permeation tests, the same tissue can be recovered for histological analyses at the end of the experiment. To this end, Basu et al. used this protocol to assess the safety of their gel formulations containing either Carbopol® 934P, sodium alginate or a combination of both excipients for venlafaxine nasal delivery (Basu and Maity, 2012). Following a fixing-staining step, the tissues recovered were compared to an unexposed mucosa that was a reference. The formulations' safety was confirmed, with no apparent necrosis.

It is thus possible, from a single permeation test, to provide a plethora of information related not only to the diffusion profile of the drug but also to the safety of the formulation.

4.1.3. *In vitro models*

Even if the *ex-vivo* model described previously offers a lot of benefits including the use of a real nasal tissue rather than a model that mimics it, it also has a few limitations. Indeed, between species, many variations can be observed in terms of tissue thickness and metabolic enzymes (with both differences in activity but also types of enzymes.) (Ehrhardt and Kim, 2008). This therefore makes the *ex vivo / in vivo* extrapolation more complicated. Moreover, the experimental parameters frequently differ between scientific studies with experimental temperatures, stirring conditions and dissolution media varying form one study to another. The data resulting from such experiments as thus difficult to compare.

In this context, it is sometimes appropriate to work with a more standardized model such as cell culture models. These *in vitro* models are easier to use in routine testing than excised tissues, which present higher variability between species and donors in terms of thickness or enzymatic activity (Schmidt et al., 1998). Both primary and immortalized cells may be used.

4.1.3.1. Primary cells. Primary cells are cells collected from a donor and then cultivated using *in vitro* cell culture conditions. The cell collection site is mainly guided by the considered pathway: local, systemic or nose-to-brain delivery. For both local and systemic applications, the medium or inferior turbinates are good choices as the respiratory mucosa is well-represented (Schmidt et al., 1998). For nose-to-brain delivery, olfactory mucosa was easily generated after withdrawing primary cells from the olfactory region of rat noses, thus making the olfactory mucosa a sampling site of choice for nose-to-brain delivery (Gartziandia et al., 2016). The researchers defined specific criteria for establishing an olfactory mucosa: an inoculation density $> 5 \times 10^5$ cells/insert ($0.9\,cm^2$) as well as TEER values $> 160\,\Omega.cm^2$ after 21 days of culture. The integrity of the layer was confirmed by the non-diffusion of carboxylated particles (< 0.001%). The extracted cells were confirmed as being olfactory cells due to the expression of 5-AC mucins.

The main limitations of using human donors are: the need for ethical protocols, the low cell differentiation, the limited number of subcultures possible, the high TEER values and a significant risk of contamination (e.g. fungal or bacterial) (Lee et al., 2005; Reichl and Becker, 2012; Yoo et al., 2003; Wu et al., 1985; Park et al., 2016). However, these primary cells present the advantage of differentiating into a tissue with a heterogeneous cell composition histologically close to that of the nasal mucosa (Hirst et al., 2014). Additionally, the characteristics of the donor (e.g. age, sex, health status) can be known and specific types of cells, for example with a diseased state, can be obtained. The variability between donors is usually considered as a factor that decreases the quality of the test as it represents a lack of standardization (Ulm et al., 2016). However, for medically oriented studies involving a large and varied sample of patients, this can be an asset thanks to the diversity of information provided (Hirst et al., 2014). A higher standardization may be achieved with commercialized primary cells such as EpiAirway™, a 3D precultured tissue model available for respiratory research and developed by MatTek Corporation (Aschland, MA). The model is derived from human tracheal/bronchial epithelial cells and contains both ciliated and non-ciliated cells, goblet cells that produce mucus and epithelium that presents tight junctions (Babu et al., 2008; Ren and Daines, 2011).

For primary-cell culture, the chosen materials for insert membranes have often been polytetrafluoroethylene (PTFE) coated with collagen for better spreading and attachment or polyester membranes, combined with the bronchial epithelial growth medium (BEGM) as the culture medium (Lee et al., 2005). The cell seeding density in inserts is usually around $5–7 \times 10^5$ cells/cm^2. The switch from liquid-covered culture (LCC) to ALI can be made 2 days after inoculation on inserts (Lee et al., 2005; Schögler et al., 2017). As with immortalized cells, the ALI configuration is essential for the establishment of cell polarization. An interesting work underscored that the formation of tight junctions and the cilia beating were apparent 4 weeks after culture under ALI conditions (Ong et al., 2016).

4.1.3.2. Immortalized cells. An alternative to primary cells is the use of immortalized cells. They present the advantage of better standardization and can be used more easily in routine testing as they are easily amplified and cultured (Reichl and Becker, 2012; Ulm et al., 2016; Kreft et al., 2015). However, immortalization can sometimes cause the appearance of unwanted morphological changes in the cell line (e.g. absence of cilia beating) (Van der Walle, 2011). Up to now, the only nasal immortal cell line of human origin available has been the RPMI 2650 cell line (Bai et al., 2008). However, other cell lines have been used for nasal application: Calu-3 and 16HBE (Bernocchi et al., 2016). Interestingly, heterogeneous tissues can be constructed from immortalized cells by developing co-cultures (e.g. RPMI 2650 cells with fibroblasts) (Wengst and Reichl, 2009).

RPMI 2650 cell line. RPMI 2650 cells were isolated from anaplastic

squamous cell carcinoma in the nasal septum (Moore and Sandberg, 1964). Their major differences with the nasal mucosa are the absence of ciliary movements and multilayer cell growth (De Fraissinette et al., 1995). Despite these few differences, RPMI 2650 cells have shown a similar permeability to nasal mucosa for hydrophilic, lipophilic and large molecular weight compounds (Reichl and Becker, 2012). The model was first used for metabolic studies (e.g. degradation tests) and, subsequently, for transport experiments after culture optimization (Gonçalves et al., 2016; Kim et al., 2018; Shin et al., 2004). In fact, RPMI 2650 cells were subject to strong histological modifications when switching from LCC to ALI (e.g. polarization, differentiation) (Reichl and Becker, 2012; Bai et al., 2008). In 2014, Pozzoli et al. conducted a study focused on non-optimized parameters for RPMI 2650 culture (e.g. inoculation density) (Pozzoli et al., 2014). It appeared that the LCC/ALI switch was feasible 24 h after inoculation when starting from a seeding density of 4–5 × 10^5 cells/cm^2 (Pozzoli et al., 2014). Cell differentiation and the presence of tight junctions were effective after two weeks under ALI conditions, with TEER values of 50 and 120 Ω.cm^2 after 1 and 2 weeks, respectively (Kim et al., 2018; Pozzoli et al., 2016a,b).

For insert materials, polyethylene terephthalate or polyester (which can be sometimes coated with collagen) are preferred for RPMI 2650 culture (Lungare et al., 2016; Gonçalves et al., 2016). The culture media selected are minimal essential medium non-essential amino acids or Eagle's modified essential medium supplemented with 10% v/v foetal bovine serum and other additives (e.g. glutamine, antibiotics) (Kreft et al., 2015; Thomas et al., 2007; Albano et al., 2016).

Calu-3 cell line. Calu-3 cells are isolated from lung adenocarcinoma and differentiate in a mixed phenotype of both ciliated and mucus-secreting cells. Therefore, a Calu-3 monolayer presents some morphological similarities (i.e. cilia, mucus production and the presence of tight junctions) with nasal tissue (Witschi and Mrsny, 1999). In addition, Calu-3 cells present similar electrical properties, with a TEER of ~100 Ω.cm^2 in ALI configuration in comparison to ~70 Ω.cm^2 for human nasal mucosa, (Shen et al., 1994; Cremaschi et al., 1997). The ALI culture conditions (Fig. 4) allow Calu-3 to be polarized and to form apical microvilli (Wan et al., 2000; Mathias et al., 2002).

Usually, Calu-3 cells are cultivated on various membrane materials (e.g. polyethylene terephthalate or PTFE (Wang et al., 2016) coated with collagen (Zhang et al., 2016) and polyester (Seki et al., 2007), with a seeding density of 4–5 × 10^5 cells/cm^2 (Wang et al., 2016; Grainger et al., 2006). An example of Calu-3 application is their wide use to study the reversible opening of tight junctions caused by chitosans, an excipient used very commonly in the intranasal field (Salade et al., 2017; Ye et al., 2013; Scherließ and Trows, 2011).

The Calu-3 cell line has also been used to assess puerarin diffusion in the presence of paeoniflorin and menthol (Zhang et al., 2016). Paeoniflorin did not show any effect, while menthol involved tight junctions opening and an alteration of the barrier integrity. Results were expressed in terms of the apparent permeability coefficient "P_{app}", which reflects the uptake efficiency of a drug through a defined barrier (Bittermann and Goss, 2017). The P_{app} of puerarin alone (1.226 ± 0.039 × 10^{-6} cm/s) was increased following the incorporation of 15, 30 and 60 µg/mL of menthol, with a P_{app} of 1.285 ± 0.084 × 10^{-6} cm/s, 1.639 ± 0.085 × 10^{-6} cm/s and 1.789 ± 0.087 × 10^{-6} cm/s respectively. By using the Calu-3 model they concluded that the puerarin transport occurred mainly by passive diffusion but also that the combination with menthol increased the passive paracellular transport by opening the tight junctions in the Calu-3 monolayer.

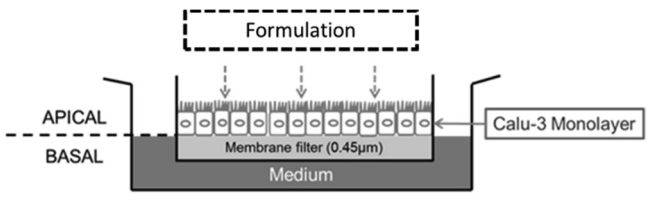

Fig. 4. Illustration of the ALI for Calu-3 cell culture.

Other researchers investigated the diffusion of losartan with or without dimethyl-β-cyclodextrin (DM-β-CD) and glycocholate (Amoako-Tuffour et al., 2009). The initial flux of losartan (P_{app}: 1.3 ± 0.5 × 10^{-6} cm/s) was not radically changed by the addition of DM-β-CD, while glycocholate (1% w/v) involved an increase in the P_{app} (8.7 ± 1.1 × 10^{-6} cm/s). The RPMI 2650 model was thus useful to show the permeation enhancer effect provided by glycocholate.

To summarize, the choice between primary and immortalized cells will be based on the information sought. At the early stage of a development, the formulator will usually evaluate several formulations and compare the effects of several excipients. In this context, it is advisable to work with a well-standardized model to avoid any additional variabilities. Therefore, the choice to work with immortalized cells seems more rational as the variability encountered with primary cells or excised nasal mucosa can be problematic. Once the most promising formulations are selected, the study can still be enriched with additional data generated through primary cell-based models or *ex vivo* models, which are closer to the true nasal mucosa.

4.2. Characterization of the formulation interaction with the nasal mucus

Once the formulation is delivered in the nose, it will be deposited in the nasal cavity and will be exposed to the mucociliary clearance, which will reduce its residence time. However, specific conditions such as disease, temperature/humidity changes or specific excipients may decrease or increase the viscosity of the mucus, impacting the elimination of the formulation.

4.2.1. Evaluation of the dripping with simulated nasal mucus

Very fast dripping of the formulation can make it flow outward from the nasal cavity (at the entrance to the nose) or flow rapidly towards the throat, which may result in a bad taste for the patient (Pu et al., 2014). This will depend on the nasal mucus state and the viscosity of the formulation. In healthy conditions, nasal mucus is about 15 µm thick and is secreted at a flow rate of 2 L per day in humans (Wilson and Allansmith, 1976). The mucus fluidity can be influenced by many factors, such as the use of mucolytic agents (e.g. N-acetyl-L-cysteine) that decrease the mucus viscosity or a diseased state such as a chronic sinusitis that involves mucus thickening (Rochat et al., 2004; Rhee et al., 1999; Akamizu et al., 2004; Dulfano and Adler, 1975; Majima et al., 1990; Majima et al., 1999; Gudis et al., 2012). Therefore, several rheological parameters may be used to study and characterize the mucus in specific conditions (e.g. pourability, viscosity, elasticity, adhesiveness and spinability) (Passali et al., 1995). In this context, it can be relevant to expose the formulation of interest to artificial mucus mimicking specific conditions (e.g. sinusitis, rhinitis).

To that purpose, an *in vitro* experiment was proposed by Masiuk et al. (2016). They established two distinct mucus compositions: a healthy one contained mucins and electrolytes, while a "diseased" one, which was more viscous and intended to mimic a chronic sinusitis, contained a saline solution to which was added locust bean gum mixed with sodium dodecyl sulphate (Anwarul Hasan et al., 2010).

The test consisted of triggering the nasal device at 3 cm from a perpendicularly oriented thin layer chromatography plate coated with the mucus of interest (Fig. 5). Afterwards, the plate was positioned vertically to assess the dripping. Coloured dyes (i.e. allura red AC, methylene blue, alcian blue GX, congo red and crystal violet) were added to the formulations to provide a better visualization. Both dripping distance and speed were recorded after a predefined time lapse, while a digital camera allowed the test to be visualized (Masiuk et al., 2016). They showed that by increasing the Avicel® concentration, a

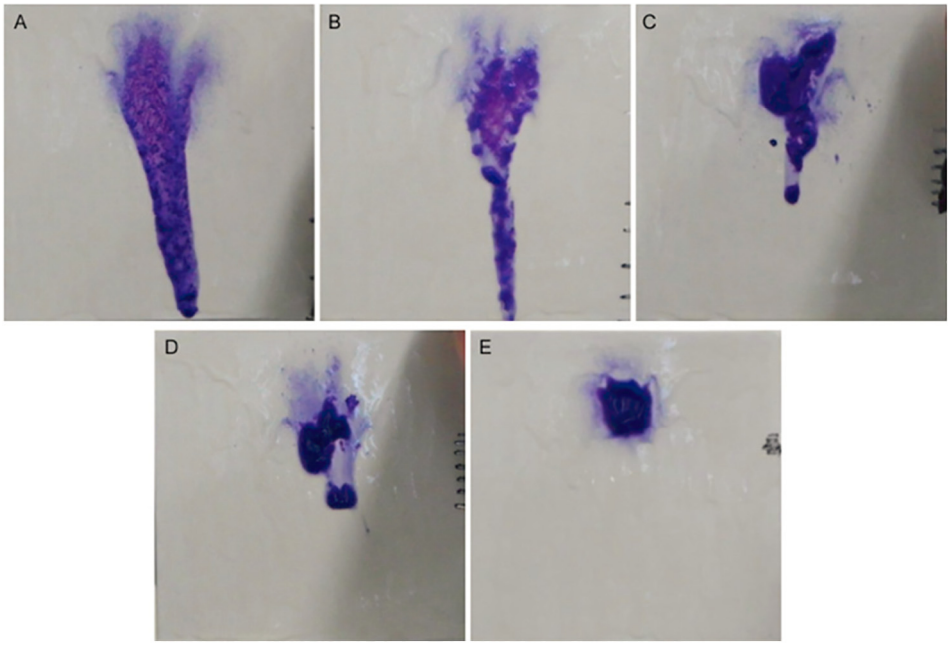

Fig. 5. Images of (A) 1%, (B) 1.5%, (C) 2%, (D) 3% and (E) 3.5% Avicel® formulations at 30 s after actuation on a thin layer chromatography plate coated with healthy simulated mucus (Masiuk et al., 2016).

thickening of the formulation was obtained and that this resulted in the reduction of the flow tendency of the formulation. The dripping was shown to be faster with the diseased mucus than with the healthy one. This was explained by the similar viscosity of the formulations and the healthy mucus compared to that of the sick mucus, which was so viscous that the formulation could flow along it.

However, this test does not consider some specific features of the nose (i.e. nasal ambient heat/humidity and mucociliary clearance). Therefore, other techniques can be more relevant (see section 4.2.2B. on mucoadhesion with nasal tissue-based models).

4.2.2. Evaluation of the mucoadhesion

The nasal mucociliary clearance is a major issue for nasal delivery as it can reduce the residence time of a liquid or powder formulation to 15–20 min (Illum, 2006). To counterbalance the clearance of the drug, both adhesive and gelling excipients may be added to the formulation to increase bioadhesion by thickening, electrostatic attraction or via specific receptor interactions (Pathak, 2011). Despite this positive effect, it is important to avoid interfering directly with the mucociliary clearance as it can render the nasal cavity more vulnerable to external contaminants (Merkus et al., 1998).

Even if certain excipients have the ability to adhere to the mucosa, the drug still has to diffuse through the mucus before reaching the nasal epithelium. This can be an issue. The mucus has been described as a double-mechanism filter (Sigurdsson et al., 2013). The first mechanism works like a sieve that prevents too-big particles from diffusing. The second mechanism is based on interactions with the particle surface. This will let particles diffuse according to their charge or/and polarity. It has been observed that by developing small nanocarriers combined with an encapsulating polymer, it is possible to increase the diffusion in the mucus (Sonvico et al., 2018). Indeed, polymers such as polyethylene glycols allow particles to avoid interactions with mucus mucins and thus to achieve a better mucopenetration.

4.2.2.1. Models with mucins. Nasal mucus consists of 95% water, 2.5–3% mucins, and a remaining 2% composed of electrolytes, proteins, lipids, enzymes and antibodies (Dondeti et al., 1996). Mucins are strongly represented glycoproteins that are negatively charged at the physiological pH of the nose. Therefore, they are the target of choice for many excipients whose role is to extend the period of contact of the drug with the mucosa (Kaliner et al., 1984). The mechanism may involve electrostatic interaction between the anionic mucins and the excipient positively charged at nasal pH (e.g. chitosan). Mucoadhesion was even defined by Leung et al. as an interaction between the mucin surface and a polymer (synthetic or natural) (Leung and Robinson, 1987).

A first method for evaluating mucoadhesion with mucins was adapted from Conte et al. by Gavini et al. (Gavini et al., 2005; Yarragudi et al., 2017; Pavanetto et al., 1994). A filter paper is soaked in a mucin solution (bovine submaxillary glands mucins 2% w/v) to become saturated with glycoproteins. Then, the filter is recovered and the formulation is dropped on it. An air stream (flux = 6.37 $m.s^{-1}$) is applied horizontally onto the filter to simulate the nasal flow and to remove unattached particles.

Gavini et al. studied the adhesion of metoclopramide-loaded microspheres produced by spray-drying and combined with either alginate, chitosan or both of them (Gavini et al., 2005). Following the application of the airflow, the filter was washed with water to quantify the drug entrapped in the microspheres that were retained on the filter. Another version of this test was proposed, with fluorescent dextrans added to microparticles to allow easier quantification without needing any solubilization step (Yarragudi et al., 2017).

A second method described the preparation of an agar/mucins mixture that was coated onto a glass plate and left for gelification (Lungare et al., 2016; Bertram and Bodmeier, 2006). The formulation is then deposited on the plate and the displacement factor is measured (Nakamura et al., 1996). This displacement factor is defined as the distance in centimetres measured between the initial deposition site of the formulation and its position at the moment of measurement (Farid et al., 2013). The mucoadhesion is thus inversely proportional to the displacement factor. Such configuration was used to characterize mucoadhesive nasal inserts based on various bioadhesive polymers and loaded with oxymetazoline HCl (Bertram and Bodmeier, 2006). The displacement of the inserts on the agar/mucin gel was evaluated to assess potential bioadhesion. This method was also used to evaluate the mucoadhesion of nasal *in situ* gelling inserts containing salbutamol (Farid et al., 2013) or liquid formulation containing amantadine and a thermosensitive polymer (Lungare et al., 2016). This method therefore

makes it possible to measure easily the potential of a formulation to adhere and to compare different excipients with each other.

A last model is based on the indirect quantification of mucins bound to the formulation. The method is based on a colorimetric quantification of glycoproteins with the reagent couple periodic acid/Schiff reagent (Mantle and Allen, 1978; Patil et al., 2010). Prior to adhesion tests, a calibration curve is established with various dilutions of mucins (e.g. 0.1, 0.25 and 0.5 mg/mL) and quantified at 560 nm with a UV-spectrophotometer. The defined amount of formulation is introduced into the test solution of mucins in a range of 0.5–1 mg/mL (Chen et al., 2013; Pawar et al., 2010). The mixture is left for 1–2 h and centrifuged to separate the mucin-formulation complexes from free mucins (Kulkarni et al., 2016). Unfixed mucins are quantified in the supernatant following incubation with periodic acid. The Schiff reagent is incorporated, and the absorbance is measured at 560 nm 30 min after the addition of the reagent. By calculating the difference in the amount of unfixed mucins with the initial amount of mucins, the amount of fixed mucins can be indirectly determined.

This method was selected to highlight the mucoadhesion when developing resveratrol-loaded microparticles with either PLGA or a PLGA/PEG combination. With the PLGA/PEG combination, 81.96 ± 1.86 µg of mucins per mg of microparticles were fixed, while PLGA microparticles showed a lower binding of 70.13 ± 2.18 µg of mucins per mg of microparticles (Lee et al., 2017). This test was therefore very useful to show the interest of the combination of both excipients. Another study compared chitosan and glycol chitosan nanoparticles for the nasal delivery of hepatitis B vaccine. Data collected showed that glycol chitosan nanoparticles could fix 0.447 mg of mucins/2 mg of nanoparticles. With chitosan nanoparticles, only 0.338 mg of mucins/2 mg of nanoparticles were bound (Pawar and Jaganathan, 2016). The glycol chitosan derivative thus appeared to be more mucoadhesive than classical chitosan.

In conclusion, different methods involving mucins are available but each uses a specific protocol. The first technique with the filter saturated with mucins involves a direct quantification of the drug. The second method with the coated glass plate instead assesses the rheological/flow properties of the formulation. The third method uses an indirect quantification of mucins fixed. Among these, the first method may be considered as the most reliable since it directly determines the amount of drug retained on the coated filter. Moreover, the application of an airflow allows a better simulation of real nasal administration.

4.2.2.2. Models with nasal tissue. Other models are based on the use of nasal tissues as the membrane of contact with the formulation. The first protocol evaluates the mucoadhesion by the "falling liquid film" technique (Fig. 6) (Kulkarni et al., 2016; Rao and Buri, 1989). The membrane used is usually sheep nasal mucosa (Nagda et al., 2011) or goat intestinal mucosa (Jain et al., 2004). The tissue is positioned at 45° and the formulation is dropped on the mucosa. A buffer (e.g. phosphate buffered saline pH 6.4, 37 °C) is perfused on the mucosa by means of a peristaltic pump with a fixed flow rate (Jain et al., 2004; Swamy and Abbas, 2011). The drug is quantified in the perfusate and the amount retained on the tissue is determined by difference (Jain et al., 2009). The number of particles adhered to the mucosa can also be evaluated by counting them with a microscope at the beginning and at the end of the test (Patil and Murthy, 2006).

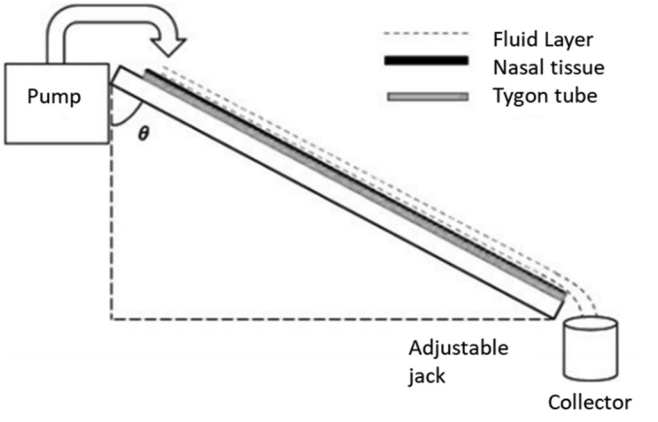

Fig. 6. Illustration of the "falling liquid film" technique (adapted from Yu et al. (2014), reproduced with authorization).

This method was used to assess the beneficial effect of increasing the chitosan/drug ratio in amlodipine besylate-loaded microspheres (Patil and Murthy, 2006). The mucoadhesion of chitosan was expressed as a percentage using the following formula (Eq. (2)):

$$Na = \frac{N}{N_0} x100 \tag{2}$$

where Na is adhesion number, N_0 is the total number of particles in a particular area and N is the number of particles remaining on the mucosa after washing. The mucoadhesion was thus enhanced by increasing the chitosan/drug ratio from 1:1 (61.21 ± 4.21%) to 5:1 (70.43 ± 1.89%). Another version of this test was proposed with the monitoring of the microspheres' weight rather than their number (Jain et al., 2004; Takeuchi et al., 1996). The mass of microspheres that did not adhere to the mucosa was determined following a centrifugation/drying procedure and used to measure the mucoadhesion (Eq. (3)):

$$\%\ mucoadhesion = \left(\frac{(weight\ \ of\ \ sample - weight\ \ of\ \ detached\ \ particles)}{weight\ \ of\ \ sample} * 100 \right) \tag{3}$$

In this study, the authors also concluded that the mucoadhesion properties were higher when the hydroxypropyl guar/amlodipine besylate ratio was increased from 1:1 (75.94 ± 0.076%) to 4:1 (80.70 ± 0.210%) (Swamy and Abbas, 2011).

A second method, called the "wash-off technique", involves the use of an instrument recommended by the US Pharmacopeia for disintegration tests (Banik et al., 2012; Meeting at Washington, 2004; Kashikar et al., 2014). Briefly, a goat intestinal mucosa is fixed on the arm of a tablet disintegration test apparatus and a known number of microparticles is spread onto the tissue. Then, the tissue is subjected to up and down movements in a selected dissolution medium. The number of remaining particles is counted at predefined times and is correlated to the mucoadhesive properties of the formulation. A manual version of this method was also proposed by Colombo et al. (2016). A rabbit nasal mucosa was left for 20 min in contact with the formulation before being washed by up and down manual movements in successive washing baths filled with a simulated nasal buffer. The recovery baths were centrifuged and the detached particles were dissolved for quantification.

A third test that uses nasal tissue for mucoadhesion assessment involves the use of a texture analyser apparatus (Fig. 7). The nasal mucosa is attached to the upper part of the instrument while the lower part is loaded with the formulation (Hägerström and Edsman, 2001; Pathak et al., 2014).

The upper arm is lowered in the formulation with a specific force (e.g. 0.1 N) during a limited period of time (e.g. 5 min) to establish an intimate contact between both elements. After that, the force required to separate both parts is recorded. This method allowed the characterization of a mucoadhesive gel loaded with venlafaxine hydrochloride. The combination of Carbopol® 934 and sodium alginate in the gel provided the highest mucoadhesion (19.25 ± 0.55 g) in comparison with gels containing, separately, Carbopol® 934 (16.39 ± 0.89 g) or sodium alginate (17.00 ± 0.87 g) (Basu and Maity, 2012). A synergic action was thus obtained with the combination of Carbopol® 934 and sodium alginate.

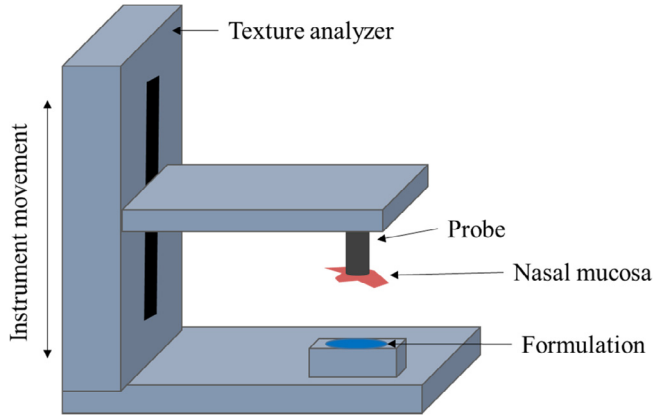

Fig. 7. Illustration of the texture analyzer apparatus equipped for mucoadhesion tests.

Using the same test, Pathak et al. showed that their mucoadhesive microemulsion provided the same adhesion to the mucosa as Carbopol®934P. This example shows that this technique may be used to compare the formulation developed against a reference (i.e. Carbopol 934P) and thus confirm that it has the same ability to adhere to the mucosa. The formulation was considered as suitable for the nose-to-brain delivery of nimodipine (Pathak et al., 2014).

4.2.2.3. Other methods. Other techniques describing the use of rheological measurement for determining the mucoadhesion have also been developed. The formulation of interest is put into contact with physiological mucus and the viscosity is then recorded after a defined period of incubation. With mucoadhesive formulations, an increase in viscosity can be observed.

A group of researchers developing *in situ* gelling systems for nasal delivery measured the viscosity of their formulation in presence of porcine intestinal mucus (500 mg of porcine mucus added to 500 µL of formulation in 100 mM phosphate buffer pH 6.8) (Menzel et al., 2017). After various incubation periods (0, 30 and 120 min), samples were analyzed with a plate-plate viscometer. For each viscosity measurement, the value of the control (mixture "phosphate buffer – formulation") was subtracted to the viscosity measured.

4.3. Determination of the formulation tolerance

Even if the addition of some excipients can easily be justified, scientists should be able to prove their safety, (Ingels et al., 1991; Schipper et al., 1991). Most frequently, the mucosa used for tolerance evaluations are not nasal mucosa but rather toad palate mucosa41, (Xie et al., 2006; Zhang et al., 2005; Gu et al., 2016). The test is usually performed on excised tissue but an alternative method is to deliver the formulation *in vivo* and recover the tissues after the animal sacrifice (Ument Karasulu et al., 2008). After exposure to the formulation, the mucosa is analyzed by optical microscopy and compared to both negative (e.g. phosphate buffer) and positive controls (e.g. isopropyl alcohol) (Shah et al., 2016). Isopropyl alcohol is a well-known toxic agent and positive control that involves cilia damage (Ohashi et al., 1988; Gao et al., 2006).

Such experiments were performed by Patel et al. to confirm tolerance of their formulations containing carbamazepine (Fig. 8). Two microemulsions were tested: a non-adhesive formulation that consisted of 6% w/w oily phase (Labrafil® M1944 CS), 32% w/w surfactant mixture (Cremophor® RH 40: Transcutol® P) and 62% w/w aqueous phase, while the adhesive formulation had the same composition plus 0.5% w/w polycarbophil. The test proved the harmlessness of both formulations and therefore their potential application as a nasal treatment.

The method has also found application for other formulations such as a nasal antihypertensive treatment containing nebivolol (Gao et al., 2006). By performing this test, the different generally recognized as safe (GRAS) excipients incorporated in the microemulsion were considered as safe, while no damage was observed on the mucosa. In another work, the same conclusion was made regarding the tolerance of a nanoemulsion containing saquinavir against HIV-1 virus (Nemichand and Laxman, 2016; Mahajan et al., 2014).

The previous analysis can be supplemented by the evaluation of ciliary movements that reflect the toxicity of a formulation (Gao et al., 2006). For example, the nasal ciliary beat frequency is a parameter that can be followed to evaluate the toxicity of cigarette smoke on the nasal mucosa (Stanley et al., 1986). The ciliary beating frequency can be measured using high-speed digital cameras and compared to the physiological beating frequency, which is around 10–12 Hz (Caruso et al., 2007). The cilia morphology may also be visualized by microscopy and their integrity can subsequently be discussed.

Another option to assess the tolerance of a formulation involves the deposition of elements (e.g. seeds) onto the mucosa following exposure to the formulation. The cleaning rate of the element spread onto the mucosa is then followed. Results are compared and discussed with regards to the physiological displacement rate (10 mm/hour) (Gizurarson, 2015). The classical protocol involves the exposure of the mucosa to the formulation as well as to a negative control (e.g. PBS pH 6.4) for 5 min. In this protocol, opium seeds are spread on the tissue and the time required for the seeds to travel a 6-mm distance is recorded (Naik and Nair, 2014; Fló-Neyret et al., 2001). This test was used to characterize a thermoreversible biogel for nose-to-brain delivery of doxepin (Naik and Nair, 2014). A gelling system combining chitosan, glycerophosphate and polyethylene glycol 4000 showed an opium-seed clearance time that was twice as long as for an untreated palate. Moreover, the gel containing only chitosan and glycerophosphate induced a complete stop of the cleaning. The formulation thus showed a strong effect on the cleaning mechanism of the nose.

5. Aerosol characteristics and performances

5.1. Determination of the size distribution

For both powders and liquids, the reference method for assessing the size distribution in the formulation is laser diffraction (Mitchell et al., 2006; Dayal et al., 2004; Guo and Doub, 2006; Guo et al., 2008; Liu et al., 2010; Inthavong et al., 2008). This method is adapted to both nano- and micrometer size ranges. However, other techniques such as dynamic light scattering are more suited to evaluating the size distribution in the nano size range. For instance, it can be relevant to compare the particle size distribution (PSD) of a powder directly after the production process (e.g. spray drying) and in the aerosol generated from the nasal device. Such a procedure allows highlighting of a potential agglomeration during storage in the device or even the ability of the device to disperse particles. Similarly, for liquid formulations, the size of the dispersed particles, in a suspension for example, can also be crucial as the particle size can influence the dissolution rate (Niazi, 2015). Size analysis reports usually includes the following parameters: D10 (diameter where 10% of the population resides below this value), D50 (diameter where 50% of the population resides below this value), D90 (diameter where 90% of the population resides below this value), Span ((D90-D10)/D50), reflects the size distribution width) and percentage of particles/droplets smaller than 10 µm (FDA, 2002).

Once evaluated in the formulation, the aerosol PSD must be determined by laser diffraction, as is recommended in the FDA guidelines (FDA, 2003). The plume generated from the device moves through the laser beam and the size distribution of the entities can be evaluated (Fig. 9). The aerosol PSD obtained is a key parameter that will directly influence the deposition site in the respiratory tract (FDA, 2002). It is well established that particles with a diameter larger than 20 µm will

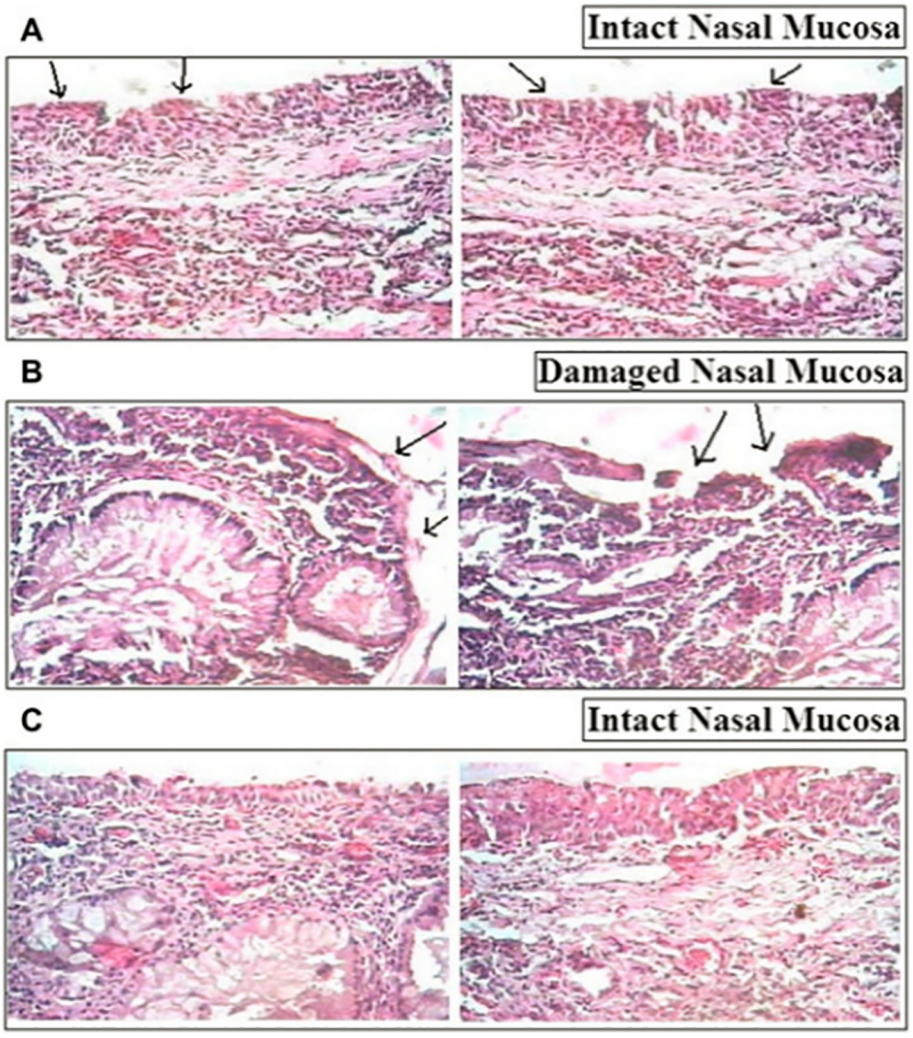

Fig. 8. Photographs of sheep nasal mucosa demonstrating histological characteristics when treated with (A) phosphate buffer saline pH 6.4, (B) isopropyl alcohol and (C) mucoadhesive microemulsion of carbamazepine (Patel et al., 2013).

Fig. 9. Nasal spray system (NSS) for standardized actuation of nasal devices combined with a Spraytec® apparatus for determination of the generated aerosol PSD by laser diffraction (reproduced with authorization © Malvern Panalytical Ltd, UK) (Spraytec Nasal Spray Support for accurate nasal spray droplet sizing from Malvern Instruments, 2018).

preferably deposit in the anterior part of the nasal cavity due to impaction, while small particles (< 5 μm) will not be stopped in the nose (El-Sherbiny et al., 2015; Shi et al., 2007) Therefore, the main size cut-off considered for nasal delivery is 10 μm. When particles or droplets are characterized by a median diameter smaller than 10 μm, they can potentially continue their journey to the lower respiratory tract by circumventing the nasal cavity (Suman et al., 1999). Additionally, it has been suggested that the best deposition in the olfactory region could be achieved with a diameter around 10 μm (Schroeter et al., 2015).

A decisive factor for such experiments is the distance between the device and the laser beam. Therefore, it is recommended to perform the PSD analysis at two different distances from the laser beam. Indeed, when the distance is modified, different parts of the plume may be evaluated (FDA & CDER, 2003). For instance, Dayal et al. observed a Dv50 decrease of 17–27% when increasing the distance from 1.5 to 6 cm between the laser beam and the device nozzle (Dayal et al., 2004). Both distances tested should be at least 3 cm apart and are usually comprised in the range 2–7 cm (FDA, 2003). However, care should be exercised when the measurement is recorded at a short distance from the device tip. Indeed, since the density within the aerosol is quite high in this area, there is a risk of underestimating the actual particles size because of the multiple scattering phenomenon (i.e. the light scattered by a droplet/particle is rescattered by another one). Dayal et al. reported that multiple scattering is likely to appear when the light transmission is 80% (Dayal et al., 2004). They therefore suggest taking into account the level of light transmission in order to avoid such bias during size measurements. When the experimenter wishes to study the size distribution at the output of the device, other more appropriate

techniques make it possible to dispense with the multiple scattering. Among these we can cite the particle/droplet image analysis (PDIA) which is based on the image capture in the aerosol (Inthavong et al., 2012). This technique is well-suited for the near-nozzle spray characterization but requires a large amount of sample in order to collect statistically representative results.

Laser diffraction is not only limited to the evaluation of the PSD but can also provide information about the spray dynamics. Indeed, during the device actuation, three distinct phases can be distinguished: the "formation phase", the "stable phase" or "fully developed phase" and the "dissipation phase" (Kippax and Fracassi, 2003). The formation phase is characterized by the generation of a dense and concentrated aerosol associated to a rapid decrease in the laser beam light transmission (which represents the amount of light penetrating the sample) (Sangolkar et al., 2012). The stable phase is characterized by the constancy in both light transmissions through the aerosol and the size of aerosol particles. Finally, a progressive increase in the light transmission may be observed in parallel with the increase in particle size during the dissipation phase (FDA, 2003; Sangolkar et al., 2012). It is thus suggested that data generated from the fully developed phase of the spray be reported (Trows et al., 2014). However, this fully developed phase has been criticized as it is not very representative of the aerosol emission in the nasal cavity. Indeed, once delivered into the nasal cavity, the spray does not have a sufficient space in order to fully develop its plume. The size measured during this fully developed phase do not directly correlate with *in vivo* deposition.

In addition to the previous parameters described, the device actuation should be well controlled and fixed to avoid any variability and thus to produce reproducible data. Automated actuators are strongly recommended (e.g. by the FDA) (FDA, 2002) as they avoid any operator-dependent variability, which can be encountered with repeated manually hand-actuated measures (FDA, 2003; Kulkarni and Shaw, 2012). Kippax et al. conducted a study in which they compared droplet size distributions from two nasal devices after both manual and automated actuations. Their data showed that the automated actuation allowed a gain in both reproducibility and standardization of the procedure (Kippax et al., 2004).

Various parameters related to the actuation can be easily controlled with such automated stations, such as the actuation force or the time between each test (Kippax and Fracassi, 2003). Usually, the force applied for actuation is ranged between 4.5 and 6 kg, which corresponds to the usual hand actuation for an adult (Dayal et al., 2004; Trows et al., 2014; Doughty et al., 2011). Both actuation force and aerosol PSD have been shown to be inversely proportional, with a decrease in both Dv50 and Dv10 when the actuation force was increased (Dayal et al., 2004; Trows et al., 2014). Dayal et al. even showed a 37% decrease in the Dv50 when increasing the actuation force from 3 to 7 kg. The actuation force may be adapted to the device used and to the population of patients targeted (e.g. children). In this context, a study conducted by Doughty et al. focused on the actuation parameters of Flonase® spray (fluticasone propionate, GlaxoSmithKline, Research Triangle Park, NC). The purpose of the study was to compare the plume properties following an adult and a paediatric actuation, simulated with an automated station. The automatic actuator settings were fixed based on "hand data" collected from patients. For example, the actuation force was fixed at 5.8 and 3.4 kg to simulate an adult and a child manual actuation, respectively. It has been concluded that differences between adult and child actuations were observed with regards to the droplet PSD, the spray weight (mass of powder emitted from the device) and the spray pattern (Doughty et al., 2011). For example, the mean spray weight collected from children's actuation was 88.2 mg (relative standard deviation – RSD – 18.9%), while 95.0 mg (RSD 1.5%) were collected from adults' actuation. The RSD was also much higher for children's actuation. Intranasal administration can thus be subject to significant variability depending on the patient age.

More advanced automated actuators allow the determination of the actuation velocity instead of the actuation force (Grmaš et al., 2017). Some companies, such as InnovaSystems (Moorestown, NJ, USA), are specialized in automated stations and can provide both types of instrument. Pneumatic actuators, such as the MightyRunt® system, allows the experimenter to fix accurately the actuation force. Other apparatus, such the NSP UA® actuator, allow the actuation velocity to be determined and involve a more complex mechanism as well as an electric motor.

In addition to parameters previously described, the aerosol can also be influenced by physicochemical properties of the formulation (e.g. rheology, density, surface tensions) and the design of the device (e.g. the orifice shape, the metering chamber, the volume delivered) (Dayal et al., 2004). In the formulation, the addition of excipients such as surfactants or polymers has shown decreasing and increasing effects on the aerosol PSD (i.e. a smaller or larger mean diameter), respectively (Dayal et al., 2004). For instance, by increasing the concentration of CMC from 1 to 2% w/v they observed a size increase in all aerosols generated from a multitude of nasal devices. This increase was correlated to the higher viscosity.

It was even shown that by adding 0.5% (w/v) Polysorbate 80 to a solution of 2% (w/v) carboxymethyl cellulose (CMC), the Dv50 decreased from 124 ± 2 µm to 92 ± 12 µm. However, with larger amounts of Polysorbate 80, the Dv50 started to increase again. Larger amounts of surfactant induced an increase in the dynamic-viscosity, which could explain the increase in the Dv50. However, observations regarding both surfactant and surface tension effects on the size distribution have been reconsidered by different studies that could not lead to a similar conclusion (Guo et al., 2008; Trows et al., 2014). Indeed, the data collected by Trows et al. and Guo et al. rather suggested a strong influence of the viscosity while a slight effect of the surface tension on the droplet size distribution.

5.2. Aerodynamic assessments with impactors

For nasal administration, next generation impactors (NGI) coupled with expansion chambers are recommended by the FDA for the estimation of the deposition in the respiratory tract (FDA, 2003). The conventional configuration (Fig. 10) consists of an expansion chamber (in which the nasal aerosol is generated) assembled to an impactor (e.g. an Andersen Cascade Impactor, NGI, etc.) (Pozzoli et al., 2016a,b). These impactors are designed for the impaction of fine particles (< 5 µm). It is therefore usually necessary to combine an expansion chamber upstream of the impactor to allow the generation of an aerosol containing larger entities (> 10 µm). It is important that the aerosol

Fig. 10. Next generation impactor coupled with a glass expansion chamber (© Copley Scientific, UK) (Impactors for Nasal Spray Testing, 2018) (reproduced with authorization).

does not impact onto the glass wall of the chamber. Therefore, it should be sampled as a fine aerosol cloud. The expansion chamber may be defined as a glass round-bottomed flask with an entry located at 30° from the vertical axis and intended to trigger the device. An expansion chamber of 1 L is recommended by the FDA to evaluate powder aerosols as they usually have a thinner plume than liquid sprays, which require the use of larger chambers (2 or 5 L). The deposition occurring in the expansion chamber represents the nasal fraction while particles or droplets that reached the impactor represent the inhalable fine particle fraction. Once the test is completed, the drug may be quantified at each stage of the NGI to evaluate its deposition quantitatively. For such an experiment, an airflow of 15 L/min is usually applied in the instrument to simulate the inspiratory flow (Garmise and Hickey, 2008).

Pozzoli et al. used a combination of a 2 L expansion chamber with a cascade impactor apparatus E with seven stages (Westech W7; Westech Ltd., Henlow, UK). They used this configuration to draw the deposition profile of beclomethasone dripropionate from the Teijin Rhinocort® dry-powder nasal spray (Pozzoli et al., 2016a,b). They observed that 95% of drug was retained in the upper respiratory tract while only 5% could reach the lower respiratory tract. In another experiment, by Scherließ et al., a combination of a 1 L expansion chamber coupled with a NGI impactor (Copley Scientific, Therwil, Switzerland) was selected to study the deposition in the nasal cavity as well as the deposition of fine particles in the lungs (Scherlie, 2010). This allowed them to estimate the amount of drug lost in the lungs. Doub et al. studied the deposition of a nasal suspension containing beclomethasone dipropionate with an Andersen cascade impactor coupled with various dimensions of expansion chambers (1, 2 and 5 L). It was concluded that the 1 L size induced a higher variability (Doub et al., 2012).

Another recent study interestingly associated both permeation and deposition tests in one experiment (Pozzoli et al., 2016a,b). The model used was Rhinocort®, a commercially available liquid suspension of budesonide (AstraZeneca, North Ryde, NSW, Australia). RPMI 2650 cells were cultivated for 14 days on Snapwell cell culture inserts. Snapwells are specifically designed to be easily removed from the initial culture plate to another place. The cell inserts were transferred to a custom-made 2 L expansion chamber designed by 3D-printing and built with acrylonitrile butadiene styrene. This expansion chamber was connected to a cascade impactor. The modified expansion chamber allowed the attachment of 3 Snapwell inserts seeded with RPMI 2650 cells. The nasal devices were triggered in the expansion chamber and the aerosol generated could be impacted on RPMI 2650 cell layers. After this, the Snapwells were recovered and placed in 6-well plates with warmed Hank's Balanced Salt Solution for drug permeation assessment. The model has been validated by comparing the deposition performances between both a classical expansion chamber and a custom-made chamber. The epithelium integrity was confirmed by performing a sodium fluorescein (a paracellular marker) permeation study with a VP3 spray pump (Aptar, Le Vaudreuil, France) (Pozzoli et al., 2016a,b). A similar study was performed by Martignoni et al. for the delivery of solid lipid microparticles containing resveratrol (Martignoni, 2016).

These expansions chambers have therefore been widely characterized, modified and, subsequently, used for the characterization of nasal sprays. However, their correlation with the anatomical structure of the nasal cavity has recently been discussed (Williams et al., 2018). Indeed, the chamber's volumes (1, 2 and 5 L) is often larger than the actual volume of the human nasal cavity. This implies, for example, that the spray emitted is subject to unexpected evaporation that causes a decrease in droplets size. This can thus reduce the droplets tendency to impact on the nasal cavity walls and falsely lead the experimenter to consider them as part of the inhalable section in the lungs. In the study of Williams et al., they proposed a new metal sampling system that is more nasal representative in terms of both angle and volume (Williams et al., 2018). This preliminary study therefore paves the way for the development of new and more anatomically relevant quality control methods for nasal products.

5.3. Deposition studies in nasal cavities using a nasal cast

Nasal casts are artificial nasal cavities used to model the real nasal cavity and to assess the deposition profile of a formulation in the different parts of the nasal cavity. The main difference between nasal casts and the impactors previously described is that nasal casts allow the detailed deposition profile of a sprayed product in the nasal cavity to be drawn while impactors provide global information about the deposition in the whole respiratory tract.

Among the different databases available, medical imagery (e.g. sectioned scans (Hörschler et al., 2003; Yu et al., 1998), computed tomography or magnetic resonance imaging scans (Subramaniam et al., 1998) initially performed for the diagnosis of diverse nasal pathologies or deformations (e.g. nasal septum deviation) (Lin et al., 2014) can be a very rich and varied databank for the design of such artificial nasal cavities. Recent nasal casts obtained from the combination of computed tomography scans and 3D printing allow the manufacture of complex and biosimilar cavities (Hughes et al., 2008). In order to build the nasal cast, the raw data resulting from medical analysis are digitally converted to be compatible with 3D-printing software (e.g. DICOM files). Commonly used 3D-printing techniques here are the fused deposition modelling process (Yarragudi et al., 2017; Le Guellec et al., 2014) and polyjet technology (Xi et al., 2016a,b). Once the nasal cast is built, the test is performed by triggering the device in the artificial cavity. Then, depending on the model of nasal cast used, qualitative and/or quantitative data can be generated.

Some of the nasal casts, such as translucent casts, are limited to qualitative data due to their construction in a mono-block structure that

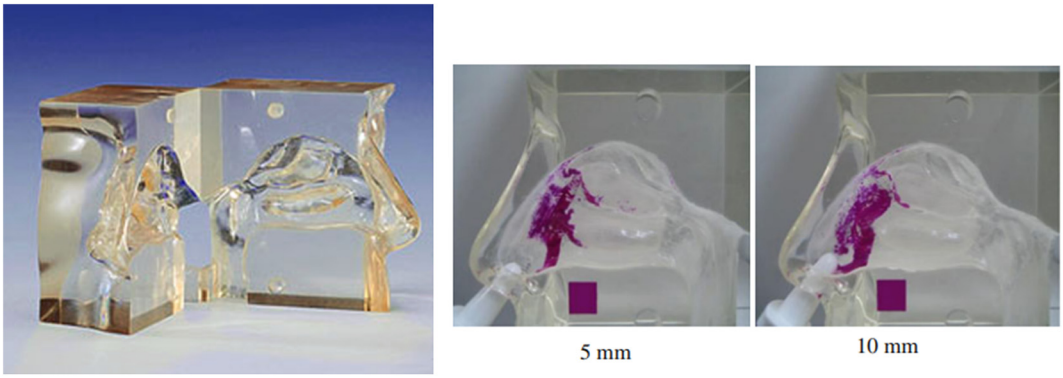

Fig. 11. Illustration (left) of the Koken® nasal cast (© Koken Co., Japan) and its use (right) for studying the effect of the device insertion depth on nasal deposition after coating the walls with Sar-Gel® (Kundoor and Dalby, 2011); reproduced with authorization).

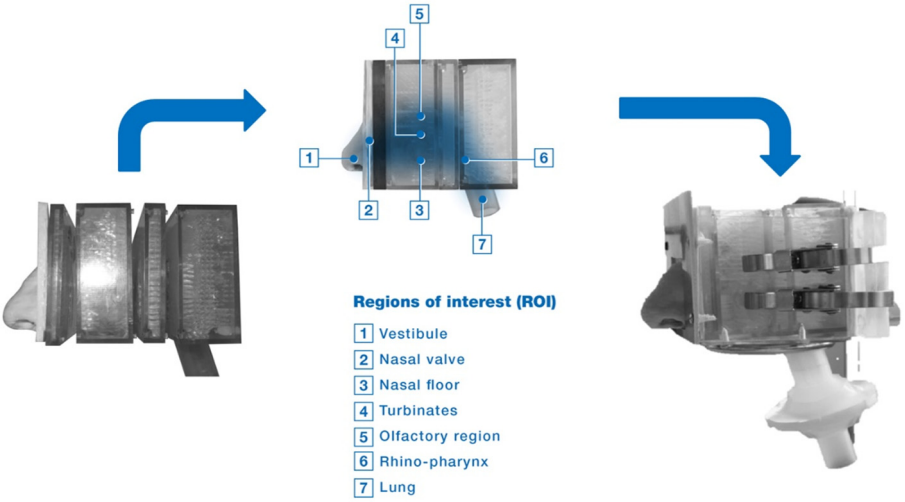

Fig. 12. Illustration of a model of a nasal cast with separable sections (© Aptar Pharma Group, reproduced with authorization).

cannot be disassembled into distinct sections (Fig. 11).

However, quantitative estimation of the deposition can also be obtained in a mono-block nasal cast by using digital camera and softwares (Kundoor and Dalby, 2011). A good visualization of a liquid formulation deposition can be achieved by coating the nasal cast with a water-indicating dye (e.g. Kolor Kut®, Sar-Gel®) (Lungare et al., 2016; Grmaš et al., 2017). Other casts can provide both qualitative and quantitative data, with anatomical models constructed in separable structures that allow quantification in specific areas (Fig. 12). Depending on the specificity needed, the cast model can be divided in 2–3 or 5–7 anatomically relevant regions. The areas of interest frequently studied are the following: nostrils, vestibule, turbinates, olfactory region and rhinopharynx. Depending on the nasal pathway targeted (e.g. local, systemic or nose-to-brain), specific areas should be targeted preferentially for deposition. For instance, when a local effect or a systemic transfer is expected, the formulation should cover the largest area of the nose to maximize the surface of contact. This may be achieved by developing a formulation with a device that is able to generate small particles or droplets as they cover a large surface.

In contrast, when a nose-to-brain transfer is considered, it is necessary to maximize the nasal deposition in a very restricted area that represents only 5.2% of the total surface of the nasal cavity, namely the olfactory mucosa (Xi et al., 2016). It is well known that the deposition of large particles or droplets (50–60 μm) occurs mainly at the entry of the nose, where this olfactory region is located (Cheng, 2001; Kundoor and Dalby, 2011; Guo et al., 2005). However, if the medium diameter is too large, the formulation can be deposited at the very beginning of the nose and can be quickly removed by sneezing or cleaning (Scherlie, 2010).

The rhinopharynx and the filter sections, located at the back of the nasal casts (Fig. 12), are the representative areas for the evaluation of losses of small inhalable particles. Indeed, the rhinopharynx section contains an aerosol part that circumvents the nasal cavity, while the filter section acts as a barrier to block the smallest particles (< 5 μm), which could theoretically continue to the deeper respiratory tract.

For the design of the nasal cast, special attention must be paid to the material selected. Ideally, the component should not be too rigid but rather flexible, stable and inert. One of the most commonly used materials is silicon. This may be found in nasal casts from Koken® or Teijin Pharma®. However, alternative materials, such as acrylonitrile butadiene styrene (Gray et al., 2016) or polypropylene (Xi et al., 2016a,b), may also be used. 3D-specific materials (e.g. VeroClear™ from Stratasys, Northville, MI) that allows the building of transparent and smooth nasal cavities are very suitable for such application.

The main disadvantage of using a nasal cast to evaluate the deposition, as well as the dispersion of a powder or liquid dispersion from a spray, is the difficulty of standardization. This is because the cast represents the nasal cavity anatomy of only one patient. Moreover, the mucociliary clearance, which is a key parameter for nasal drug delivery, cannot be evaluated in such artificial models. However, some studies included a step of moistening the nasal cast. This is performed by either nebulization or simple application of water or synthetic mucus (e.g. glycerol/surfactant mixture) prior to device actuation (Shah et al., 2014). Many parameters need to be optimized and controlled to limit unexpected variations, such as the actuation force, the tilt angle of the device, the insertion depth in nostrils and the airflow applied in the system. Therefore, studies using nasal casts should specify the values of these parameters as they can introduce bias into the test. The insertion depths of the device in the nostrils are usually around 5–10 mm and the tilt angles frequently selected are 23°, 45°, 60° and 80° (Lungare et al., 2016; Hughes et al., 2008; Kundoor and Dalby, 2011). Tilt angles of 60–75° between the base of the nasal cast and the device, combined with an inclination of 15° to represent the head forward, seem to provide a suitable pattern for the nose-to-brain pathway. This pattern has shown the highest deposition in the olfactory region (Lungare et al., 2016; Kundoor and Dalby, 2011). A tilt angle of 30° was reported as covering the widest surface of the nasal cavity, which is very relevant for systemic or local delivery (Foo et al., 2007). Similarly to other experiments involving the nasal device, the use of an automated actuator allows operator-dependent variabilities to be avoided. In contrast, with impactors, an airflow can also be applied through the system to mimic human inspiration when a breath actuated device is studied (Colombo et al., 2016). Indeed, a majority of nasal sprays even require the patient inhalation or the closure of one nostril, during administration. This aspect has been addressed in a recent scientific study by Moraga-Espinoza et al. (2018). They studied the effect of respiratory flow on both plume geometry and drug distribution in nasal cast. The tests were performed by varying the respiratory flow (0, 10 and 45 L/min) but also by administering the formulation with both nostrils open or only one. They could highlight that these parameters had a drastic effect on the nasal drug distribution. For example, by simultaneously inhaling and closing one nostril, the velocity of the drops was greatly increased in the different nasal cast studies. Due to this flow change, the drug deposition site was directly impacted (especially in the turbinate zone). It is therefore very relevant to adapt the parameters of such experiment according to the recommendations of use of the device (i.e. inhalation during administration, closing a nostril, etc.).

Nasal casts were used by Pu et al. to study the influence of

increasing the viscosity by adding microcrystalline cellulose or hydroxypropyl methylcellulose to their nasal liquid sprays (Pu et al., 2014). It was shown that the incorporation of microcrystalline cellulose (1 and 2% w/v) allowed dripping of the formulation at the front of the nose to be decreased while avoiding strong modifications of the deposition pattern.

Another experiment performed by Xi et al. focused on deposition in the olfactory region for nose-to-brain delivery. They compared different techniques for maximizing the deposition on the olfactory mucosa of the nasal cast: vestibular intubation (releasing the particles at a precise point of the vestibule), deep intubation (the nozzle of the nebulizer was placed below the olfactory mucosa) and electrically guided deposition (enhancing the deposition of charged particles in the olfactory region by applying an external electric force). It has been concluded that the electric guidance resulted in 16% deposition in the olfactory region while deep intubation provided only 1% deposition (Xi et al., 2017). Thus, experiments on a nasal cast make it possible to compare new techniques of targeted administration and thus to select the most promising. Another experiment also targeted nose-to-brain delivery but with a powder formulation containing chitosan-coated liposomes loaded with ghrelin (Salade et al., 2018). This approach adjusted the physicochemical properties of the powder developed and used the Unit-Dose System device from Aptar Pharma® (Le Vaudreuil, France). This device has been designed for optimizing the deposition in the olfactory region. With this process, it was possible to get a deposition higher than 50% in the olfactory region. Once again, the nasal cast allows confirmation that the formulation developed meets the criteria required for nose-to-brain delivery well and that the development can therefore be continued.

Finally, it must be mentioned that nasal casts can be combined with other techniques to collect complementary data. In this context, an innovative configuration was proposed with a nasal cast coupled with an NGI (Coowanitwong, 2011). Such combination is similar to the previously discussed expansion chamber-impactor set-up. However, the replacement of the expansion chamber by the nasal cast provides more detailed information about the deposition in the nose. In this way, it is possible to draw a detailed deposition profile for the entire respiratory tract.

In conclusion, deposition experiments using nasal casts appear to be a very helpful technique for comparing different nasal devices, various formulations and diverse deposition protocols. Moreover, they are very useful for estimating the drug deposition in specific areas of the nose. However, the number of nasal casts used should be greater than one or two models and should involve nasal cavities presenting widespread anatomical particularities (e.g. septum deviations) to provide easier extrapolation to a larger part of the patient population.

5.4. Assessment of the plume geometry and spray pattern

Plume geometry and spray pattern are both recommended by the FDA for pressurized metered dose nasal sprays and single-/multiple-use devices (FDA, 2002). Both tests are complementary parameters related to the plume morphology that allows visualization of the spray appearance at the exit of the device.

Both tests are easily and drastically impacted by device dependent parameters (e.g. pump design, shape of the nozzle) (Niazi, 2004), formulation characteristics (e.g. viscosity, surface tension) (Guo and Doub, 2006; Trows et al., 2014) or even by patient handling of the device (e.g. actuation force). For both techniques, data can be recorded using manual or automated image analysis (Trows et al., 2014). The main difference between the two measurements is the orientation between the spray and the measurement. The plume geometry is recorded from the side view, providing data regarding the plume angle (defined as the angle delimited by the two outer peripheral limits of the nasal spray). The spray pattern involves a cross section of the plume, focusing on its diameters and ovality (Figs. 13 and 14) (Marx and Birkhoff, 2011). Another difference between both methods is that the plume geometry is recorded at a very precise moment, while the spray pattern is recorded on the basis of a summation of images resulting from the whole spraying process (Guo and Doub, 2006).

To evaluate the geometry of the plume, the analysis should be performed during the fully developed phase of the spray (similarly to particle size measurements) and at a distance from the nozzle greater than that used for spray pattern evaluation (≥ 6 cm) (Guo and Doub, 2006; FDA, 2003; Trows et al., 2014). Therefore, the delay set to start the measurement after the spray development should be fixed during the fully developed phase. This delay fixing often requires a prior validation step (Shargel and Kanfer, 2010). The measurement in the fully developed phase ensures good reproducibility as well as stable PSD values (Trows et al., 2014). It is also recommended that the measurement is done when the plume is still in contact with the device tip (FDA, 2003). Crucial information should be mentioned in such studies, such as the visualization technique selected (e.g. a SprayVIEW™ NSP system equipped with a high-speed digital camera) (Suman et al., 2002).

For the spray pattern, the tip device-apparatus distance is also crucial and should be made at two distinct distances, between 3 and 7 cm (Pu et al., 2014; Chen et al., 2015). The technique to evaluate the pattern of the spray can be an impaction- or a non-impaction-based method. Impaction-based methods involve the deposition of the spray on a surface, usually a thin-layer chromatography plate. The visualization technique can be specific to the drug or based on the use of dyes or fluorescent additives to make the impacted formulation visible. The non-impaction-based method uses a laser sheet coupled with a high-speed digital camera. This technique presents the advantage of overcoming analyst bias (Makidon et al., 2010). Data is usually expressed in terms of spray areas, minimal (D_{min}) and maximal (D_{max}) diameters, the ovality ratio (D_{max}/D_{min}) and the shape of the pattern.

Such techniques were used to evaluate the effect of a viscosity enhancer on the plume morphology (e.g. to increase the residence time or limit sedimentation during a suspension administration) (Pu et al., 2014; Pennington et al., 2008). It was shown that an increase in the viscosity led to the production of larger particles or droplets in the aerosol, which remained in a smaller spray area and had a thinner plume (Fig. 13) (Kundoor and Dalby, 2011).

For example, Trows et al. showed that by adding 5% w/v of sodium carboxymethyl cellulose in water, the angle of the plume was decreased from 82.1° to 13.2° (Trows et al., 2014). A narrower plume angle implies the spreading of the aerosol cloud over a smaller area in the nose, which may be of interest when targeting a specific area of the nasal cavity (e.g. the olfactory mucosa). Other studies reported correlations between the spray pattern and the rheological analysis in shear thinning systems containing corticosteroid after gradual additions of microcrystalline cellulose (Pennington et al., 2008). Guo et al. reached the same conclusion regarding the viscosity and the geometry of the plume. It was therefore concluded that by varying the viscosity of the formulation, the morphological characteristics of the spray could be changed. In addition, they assessed the influence of actuation parameters on the plume. It was demonstrated that by increasing the actuation velocity, the plume angle, plume width and spray pattern area were increased (Guo et al., 2008). Other data have shown that the spray pattern is also very dependent on the nozzle device shape (Guo and Doub, 2006).

6. Conclusion

Nasal drug delivery is a route of administration that may offer many benefits over conventional administrations. Despite the simple appearance of the human nose and its easy access, the development of nasally delivered treatments requires an accurate and complete development that covers drug characterization, formulation development and aerosol evaluation to ensure optimal delivery of the pharmaceutical. Such a process allows the desired anatomic site to be reached

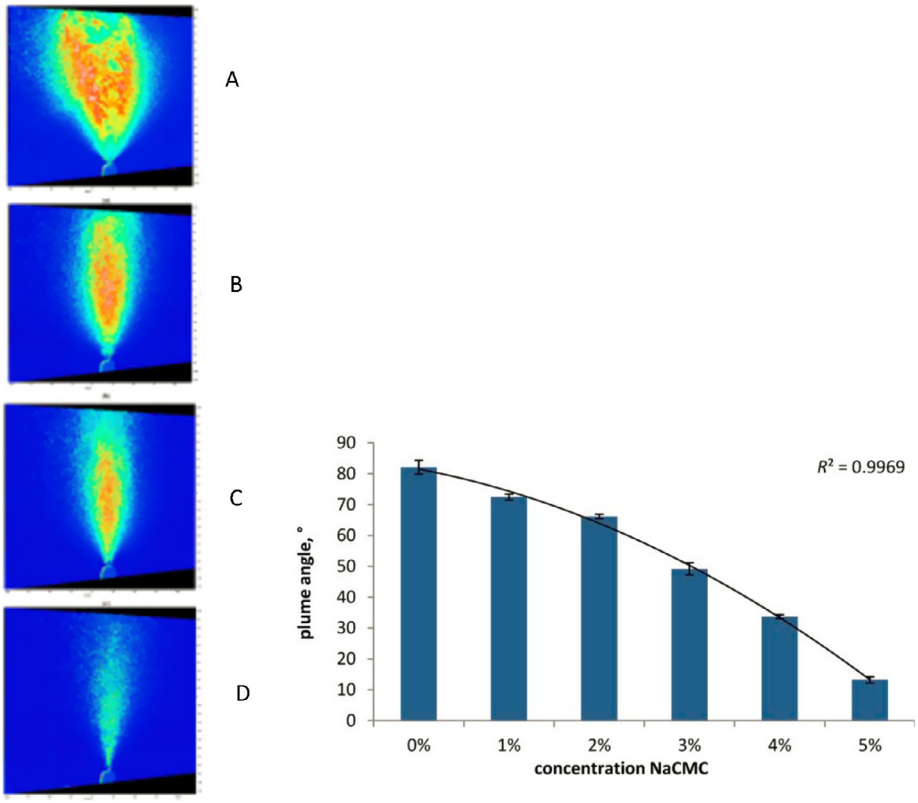

Fig. 13. Influence of the viscosity on both plume geometry and plume angle, with increased concentrations of sodium carboxymethyl cellulose (A: 0%, B: 1%, C: 2%, D: 3%) (Trows et al., 2014); reproduced with authorization).

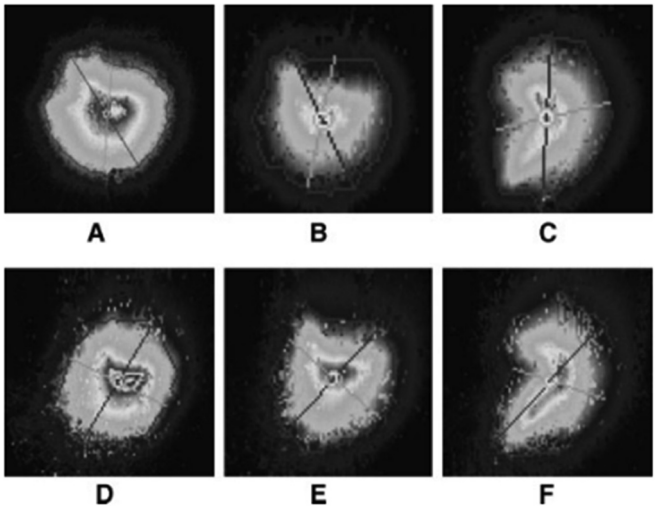

Fig. 14. Spray pattern of three different Pfeiffer® pumps (image not in scale). Spray pattern at 3 cm (A–C) and at 6 cm (D–F) for the pumps used for stroke length, actuation velocity and acceleration testing, respectively. Note that the pump used for acceleration testing has a more kidney-shaped spray pattern (Guo and Doub, 2006).

while ensuring the drug's effectiveness, minimizing side effects and limiting drug losses and degradations. The medicine developed should also show guaranteed compatibility with the human nose and that no tissue damage can be observed (Kumar et al., 2014). Thanks to recent innovations in both characterization methods and formulation technologies, it will be possible to develop promising treatments that can fully exploit the advantages of nasal administration (Bhise et al., 2008). Even if a plethora of data can be collected with *in vitro* and *ex vivo* experiments, *in vivo* experiments cannot be avoided as these are the only way to properly assess the behaviour of a formulation once it has been administered in patients (Djupesland, 2013).

Moreover, the development of new devices specifically designed for intranasal administration makes it possible to better target the nasal cavity or even specific areas of the nasal cavity. They make it possible to limit drug losses (e.g. in the lungs), deliver accurate doses and produce aerosols guaranteeing a suitable PSD for nasal delivery.

However, there are still a lot of unanswered questions in the nasal field, especially for more complex nasal pathways such as nose-to-brain delivery.

Acknowledgements

The authors would like to acknowledge Malvern Panalytical Ltd., the manufacturer of the Spraytec apparatus, for providing the illustration of the instrument.

Conflicts of interest

Author declares that there is not conflicts of interest in the present manuscript.

References

Acharya, S.P., Pundarikakshudu, K., Panchal, A., Lalwani, A., 2013. Preparation and evaluation of transnasal microemulsion of carbamazepine. Asian J. Pharm. Sci. 8, 64–70.
Akamizu, T., et al., 2004. Pharmacokinetics, safety, and endocrine and appetite effects of ghrelin administration in young healthy subjects. Eur. J. Endocrinol. 150, 447–455.
Albano, G.D., et al., 2016. Effect of high, medium, and low molecular weight hyaluronan on inflammation and oxidative stress in an in vitro model of human nasal epithelial cells. Mediators Inflamm. 2016, 1–13.
Amoako-Tuffour, M., Yeung, P., Agu, R., 2009. Permeation of losartan across human respiratory epithelium: an in vitro study with Calu-3 cells. Acta Pharmaceut. 59, 395.
Amoore, J.E., et al., 1971. Olfaction. Springer, Berlin Heidelberg.
Anwarul Hasan, M., Lange, C.F., King, M.L., 2010. Effect of artificial mucus properties on

the characteristics of airborne bioaerosol droplets generated during simulated coughing. J. Nonnewton. Fluid Mech. 165, 1431–1441.
Babu, R.J., Dayal, P., Singh, M., 2008. Effect of cyclodextrins on the complexation and nasal permeation of melatonin. Drug Deliv. 15, 381–388.
Bahamondez-Canas, T.F., Cui, Z., 2018. Intranasal immunization with dry powder vaccines. Eur. J. Pharm. Biopharm. 122, 167–175.
Bai, S., Yang, T., Abbruscato, T.J., Ahsan, F., 2008. Evaluation of human nasal RPMI 2650 cells grown at an air–liquid interface as a model for nasal drug transport studies. J. Pharm. Sci. 97, 1165–1178.
Banik, N., Hussain, A., Ramteke, A., Sharma, H.K., Maji, T.K., 2012. Preparation and evaluation of the effect of particle size on the properties of chitosan-montmorillonite nanoparticles loaded with isoniazid. RSC Adv. 2, 10519.
Basu, S., Maity, S., 2012. Preparation and characterisation of mucoadhesive nasal gel of venlafaxine hydrochloride for treatment of anxiety disorders. Indian J. Pharm. Sci. 74, 428–433.
Bechgaard, E., Gizurarson, S., Jørgensen, L., Larsen, R., 1992. The viability of isolated rabbit nasal mucosa in the Ussing chamber, and the permeability of insulin across the membrane. Int. J. Pharm. 87, 125–132.
Bernocchi, B., et al., 2016. Mechanisms allowing protein delivery in nasal mucosa using NPL nanoparticles. J. Control. Release 232, 42–50.
Bertram, U., Bodmeier, R., 2006. In situ gelling, bioadhesive nasal inserts for extended drug delivery: in vitro characterization of a new nasal dosage form. Eur. J. Pharm. Sci. 27, 62–71.
Beule, A.G., 2010. Physiology and pathophysiology of respiratory mucosa of the nose and the paranasal sinuses. GMS Curr. Top. Otorhinolaryngol Head Neck Surg. 9, Doc07.
Bhise, S.B., Yadav, A.V., Avachat, A.M., Malayandi, R., 2008. Bioavailability of intranasal drug delivery system. Asian J. Pharm. 2.
Bittermann, K., Goss, K.-U., 2017. Predicting apparent passive permeability of Caco-2 and MDCK cell-monolayers: a mechanistic model. PLoS One. https://doi.org/10.1371/journal.pone.0190319.
Borchardt, R.T., Smith, P.L., Wilson, G., 1996. Models for Assessing Drug Absorption and Metabolism. Plenum Press.
Cai, Z., et al., 2011. Formulation and evaluation of in situ gelling systems for intranasal administration of gastrodin. AAPS PharmSciTech 12, 1102–1109.
Caruso, G., Gelardi, M., Passali, G.C., de Santi, M.M., 2007. Nasal scraping in diagnosing ciliary dyskinesia. Am. J. Rhinol. 21, 702–705.
Casettari, L., Illum, L., 2014. Chitosan in nasal delivery systems for therapeutic drugs. J. Control. Release 190, 189–200.
Chaturvedi, M., Kumar, M., Pathak, K., 2011. A review on mucoadhesive polymer used in nasal drug delivery system. J. Adv. Pharm. Technol. Res. 2, 215–222.
Chen, L., et al., 2013. Enhanced nasal mucosal delivery and immunogenicity of anti-caries DNA vaccine through incorporation of anionic liposomes in chitosan/DNA complexes. PLoS One 8, e71953.
Chen, J.-A., et al., 2015. Ghrelin prevents tumour- and cisplatin-induced muscle wasting: characterization of multiple mechanisms involved. J. Cachexia. Sarcopenia Muscle 6, 132–143.
Cheng, Y.S., et al., 2001. Characterization of nasal spray pumps and deposition pattern in a replica of the human nasal airway. J. Aerosol Med. 14, 267–280.
Cingolani, E., 2017. In-vitro Investigation of Factors Affecting the Fate of Dry Powders in the Lung. University of Nottingham.
Colombo, G., et al., 2016. Nasal powders of thalidomide for local treatment of nose bleeding in persons affected by hereditary hemorrhagic telangiectasia. Int. J. Pharm. 514, 229–237.
Coowanitwong, I., et al., 2011. Regional deposition of beclomethasone dipropionate powder existing Puvlizer® in a nasal cast connected to a next generation impactor. RDD Eur. 2, 373–378.
Costin, G.-E., Raabe, H. & Curren, R., 2009. In vitro safety testing strategy for skin irritation using the 3D reconstructed human epidermis.
Cremaschi, D., Porta, C., Ghirardelli, R., 1997. Endocytosis of polypeptides in rabbit nasal respiratory mucosa. Physiology 12, 219–225.
Crouter, A., Briens, L., 2014. The effect of moisture on the flowability of pharmaceutical excipients. AAPS PharmSciTech 15, 65–74.
Csaba, N., Garcia-Fuentes, M., Alonso, M.J., 2009. Nanoparticles for nasal vaccination. Adv. Drug Deliv. Rev. 61, 140–157.
D'Souza, M.J., 2015. Nanoparticulate vaccine delivery systems. Pan Stanford Publishing.
Davis, S.S., 2001. Nasal vaccines. Adv. Drug Deliv. Rev. 51, 21–42.
Dayal, P., et al., 2004. Evaluation of different parameters that affect droplet-size distribution from nasal sprays using the Malvern Spraytec®. J. Pharm. Sci. 93, 1725–1742.
De Fraissinette, A., Brun, R., Felix, H., Vonderscher, J., Rummelt, A., 1995. Evaluation of the human cell line RPMI 2650 as an in vitro nasal model. Rhinology 33, 194–198.
Dehghan, S., Kheiri, M.T., Abnous, K., Eskandari, M., Tafaghodi, M., 2018. Preparation, characterization and immunological evaluation of alginate nanoparticles loaded with whole inactivated influenza virus: dry powder formulation for nasal immunization in rabbits. Microb. Pathog. 115, 74–85.
Djupesland, P.G., 2013. Nasal drug delivery devices: characteristics and performance in a clinical perspective—a review. Drug Deliv. Transl. Res. 3, 42–62.
Dondeti, P., Zia, H., Needham, T.E., 1996. Bioadhesive and formulation parameters affecting nasal absorption. Int. J. Pharm. 127, 115–133.
Doub, W.H., et al., 2012. Measurement of drug in small particles from aqueous nasal sprays by andersen cascade impactor. Pharm. Res. 29, 3122–3130.
Doughty, D.V., Vibbert, C., Kewalramani, A., Bollinger, M.E., Dalby, R.N., 2011. Automated actuation of nasal spray products: determination and comparison of adult and pediatric settings. Drug Dev. Ind. Pharm. 37, 359–366.
Dulfano, M.J., Adler, K.B., 1975. Physical properties of sputum. VII. Rheologic properties and mucociliary transport. Am. Rev. Respir. Dis. 112, 341–347.
Ehrhardt, C., Kim, K.-J. (Eds.), 2008. Drug Absorption Studies: In Situ, In Vitro and In Silico Models. Springer.
Ellison, R.T., Giehl, T.J., 1991. Killing of gram-negative bacteria by lactoferrin and lysozyme. J. Clin. Invest. 88, 1080–1091.
El-Sherbiny, I.M., El-Baz, N.M., Yacoub, M.H., 2015. Inhaled nano- and microparticles for drug delivery. Glob. Cardiol. Sci. Pract. 2015, 2.
England, R.J., Homer, J.J., Knight, L.C., Ell, S.R., 1999. Nasal pH measurement: a reliable and repeatable parameter. Clin. Otolaryngol. Allied Sci. 24, 67–68.
EVOM2: Instruction Manual. Word Precis. Instruments.
Farid, R.M., Etman, M.A., Nada, A.H., Ebian, A.E.A.R., 2013. Formulation and in vitro evaluation of salbutamol sulphate in situ gelling nasal inserts. AAPS PharmSciTech 14, 712–718.
FDA & CDER, 2003. Guidance for Industry Bioavailability and Bioequivalence Studies for Nasal Aerosols and Nasal Sprays for Local Action.
FDA, 2012. Guidance for Industry Nasal Spray and Inhalation Solution, Suspension, and Spray Drug Products. 20857.
FDA, 2003. Bioavailability and Bioequivalence Studies for Nasal Aerosols and Nasal Sprays for Local Action. 20857, pp. 301–827.
Fló-Neyret, C., Lorenzi-Filho, G., Macchione, M., Garcia, M.L.B., Saldiva, P.H.N., 2001. Effects of formaldehyde on the frog's mucociliary epithelium as a surrogate to evaluate air pollution effects on the respiratory epithelium. Brazilian J. Med. Biol. Res. 34, 639–643.
Foo, M.Y., Cheng, Y.-S., Su, W.-C., Donovan, M.D., 2007. The influence of spray properties on intranasal deposition. J. Aerosol Med. 20, 495–508.
Foster, K.A., Avery, M.L., Yazdanian, M., Audus, K.L., 2000. Characterization of the Calu-3 cell line as a tool to screen pulmonary drug delivery. Int. J. Pharm. 208, 1–11.
Foxman, E.F., et al., 2015. Temperature-dependent innate defense against the common cold virus limits viral replication at warm temperature in mouse airway cells. Proc. Natl. Acad. Sci. U. S. A. 112, 827–832.
Gad, S.C., Wiley InterScience (Online service), 2008. Pharmaceutical Manufacturing Handbook : Production and Processes. Wiley-Interscience.
Gänger, S., Schindowski, K., 2018. Tailoring formulations for intranasal nose-to-brain delivery: a review on architecture, physico-chemical characteristics and mucociliary clearance of the nasal olfactory mucosa. Pharmaceutics 10, 116.
Gao, X., et al., 2006. Lectin-conjugated PEG–PLA nanoparticles: preparation and brain delivery after intranasal administration. Biomaterials 27, 3482–3490.
Gardiner, Q., Oluwole, M., Tan, L., White, P.S., 1996. An animal model for training in endoscopic nasal and sinus surgery. J. Laryngol. Otol. 110, 425–428.
Garmise, R.J., Hickey, A.J., 2008. Calibration of the andersen cascade impactor for the characterization of nasal products. J. Pharm. Sci. 97, 3462–3466.
Gartziandia, O., et al., 2016. Nanoparticle transport across in vitro olfactory cell monolayers. Int. J. Pharm. 499, 81–89.
Gavini, E., Rassu, G., Sanna, V., Cossu, M., Giunchedi, P., 2005. Mucoadhesive microspheres for nasal administration of an antiemetic drug, metoclopramide: in-vitro/ex-vivo studies. J. Pharm. Pharmacol. 57, 287–294.
Gibaldi, M., Lee, M., Desai, A., American Society of health-system pharmacists, 2007. Gibaldi's Drug Delivery Systems in Pharmaceutical Care. American Society of Health-System Pharmacists.
Giuliani, A., et al., 2018. In vivo nose-to-brain delivery of the hydrophilic antiviral ribavirin by microparticle agglomerates. Drug Deliv. 25, 376–387.
Gizurarson, S., 1993. The relevance of nasal physiology to the design of drug absorption studies. Adv. Drug Deliv. Rev. 11, 329–347.
Gizurarson, S., 2015. The effect of cilia and the mucociliary clearance on successful drug delivery. Biol. Pharm. Bull. 38, 497–506.
Gonçalves, V.S.S., Matias, A.A., Poejo, J., Serra, A.T., Duarte, C.M.M., 2016. Application of RPMI 2650 as a cell model to evaluate solid formulations for intranasal delivery of drugs. Int. J. Pharm. 515, 1–10.
Grainger, C.I., Greenwell, L.L., Lockley, D.J., Martin, G.P., Forbes, B., 2006. Culture of Calu-3 cells at the air interface provides a representative model of the airway epithelial barrier. Pharm. Res. 23, 1482–1490.
Gray, E., Maducdoc, M., Manuel, C., Wong, B.J.F., 2016. Estimation of nasal tip support using computer-aided design and 3-dimensional printed models. JAMA Facial Plast. Surg. 18, 285–291.
Graziadei, P.P.C., 1971. The Olfactory Mucosa of Vertebrates. Springer, Berlin, Heidelberg, pp. 27–58 doi: 10.1007/978-3-642-65126-7_2.
Grmaš, J., Stare, K., Božič, D., Injac, R., Dreu, R., 2017. Elucidation of formulation and delivery device-related effects on in vitro performance of nasal spray with implication to rational product specification identification. J. Aerosol Med. Pulm. Drug Deliv. https://doi.org/10.1089/jamp.2016.1328.
Gu, F., Ma, W., Meng, G., Wu, C., Wang, Y., 2016. Preparation and in vivo evaluation of a gel-based nasal delivery system for risperidone. Acta Pharm. 66, 555–562.
Gudis, D., Zhao, K., Cohen, N.A., 2012. Acquired cilia dysfunction in chronic rhinosinusitis. Am. J. Rhinol. Allergy 26, 1–6.
Guo, C., Doub, W.H., 2006. The influence of actuation parameters on in vitro testing of nasal spray products. J. Pharm. Sci. 95, 2029–2040.
Guo, Y., Laube, B., Dalby, R., 2005. The effect of formulation variables and breathing patterns on the site of nasal deposition in an anatomically correct model. Pharm. Res. 22, 1871–1878.
Guo, C., Stine, K.J., Kauffman, J.F., Doub, W.H., 2008. Assessment of the influence factors on in vitro testing of nasal sprays using Box-Behnken experimental design. Eur. J. Pharm. Sci. 35, 417–426.
Hägerström, H., Edsman, K., 2001. Interpretation of mucoadhesive properties of polymer gel preparations using a tensile strength method. J. Pharm. Pharmacol. 53, 1589–1599.
Harkema, J.R., Carey, S.A., Wagner, J.G., 2006. The nose revisited: a brief review of the comparative structure, function, and toxicologic pathology of the nasal epithelium.

Toxicol. Pathol. 34, 252–269.
Hirst, R.A., et al., 2014. Culture of primary ciliary dyskinesia epithelial cells at air-liquid interface can alter ciliary phenotype but remains a robust and informative diagnostic aid. PLos One 9 (2). https://doi.org/10.1371/journal.pone.0089675.
Hörschler, I., Meinke, M., Schröder, W., 2003. Numerical simulation of the flow field in a model of the nasal cavity. Comput. Fluids 32, 39–45.
Huang, C.H., Kimura, R., Nassar, R.B., Hussain, A., 1985. Mechanism of nasal absorption of drugs I: physicochemical parameters influencing the rate of in situ nasal absorption of drugs in rats. J. Pharm. Sci. 74, 608–611.
Hughes, R., Watterson, J., Dickens, C., Ward, D., Banaszek, A., 2008. Development of a nasal cast model to test medicinal nasal devices. Proc. Inst. Mech. Eng. Part H J. Eng. Med. 222, 1013–1022.
Illum, L., 1996. Nasal delivery. The use of animal models to predict performance in man. J. Drug Target. 3, 427–442.
Illum, L., 2004. Is nose-to-brain transport of drugs in man a reality? J. Pharm. Pharmacol. 56, 3–17.
Illum, L., 2006. Nasal clearance in health and disease. J. Aerosol Med. 19, 92–99.
Illum, L., Farraj, N.F., Davis, S.S., 1994. Chitosan as a novel nasal delivery system for peptide drugs. Pharm. Res. 11, 1186–1189.
Impactors for Nasal Spray Testing. Available at: http://www.copleyscientific.com/home/inhaler-testing/aerodynamic-particle-size/impactors-for-testing-nasal-delivery-systems. (Accessed: 19th September 2018).
Ingels, K.J., Kortmann, M.J., Nijziel, M.R., Graamans, K., Huizing, E.H., 1991. Factors influencing ciliary beat measurements. Rhinology 29, 17–26.
Inthavong, K., Tian, Z.F., Tu, J.Y., Yang, W., Xue, C., 2008. Optimising nasal spray parameters for efficient drug delivery using computational fluid dynamics. Comput. Biol. Med. 38, 713–726.
Inthavong, K., Yang, W., Fung, M.C., Tu, J.Y., 2012. External and near-nozzle spray characteristics of a continuous spray atomized from a nasal spray device. Aerosol Sci. Technol. 46, 165–177.
Jain, S.A., Chauk, D.S., Mahajan, H.S., Tekade, A.R., Gattani, S.G., 2009. Formulation and evaluation of nasal mucoadhesive microspheres of Sumatriptan succinate. J. Microencapsul. 26, 711–721.
Jain, S.K., Chourasia, M.K., Jain, A.K., Jain, R.K., Shrivastava, A.K., 2004. Development and characterization of mucoadhesive microspheres bearing salbutamol for nasal delivery. Drug Deliv. 11, 113–122.
Kaliner, M., Marom, Z., Patow, C., Shelhamer, J., 1984. Human respiratory mucus. J. Allergy Clin. Immunol. 73, 318–323.
Kanojia, G., et al., 2016. A design of experiment approach to predict product and process parameters for a spray dried influenza vaccine. Int. J. Pharm. 511, 1098–1111.
Karasulu, E., Yavaşoğlu, A., Evrenşanal, Z., Uyanıkgil, Y., Karasulu, H.Y., 2008. Permeation studies and histological examination of sheep nasal mucosa following administration of different nasal formulations with or without absorption enhancers. Drug Deliv. 15, 219–225.
Kashikar, V., Dhole, S., Kandekar, U., Khose, P., 2014. Study of Mucoadhesive Microsphere of Pirfenidone for Nasal Drug Delivery. Asian J, Pharm.
Kilian, N., Müller, D.G., 1998. The effect of a viscosity and an absorption enhancer on the intra nasal absorption of metoprolol in rats. Int. J. Pharm. 163, 211–217.
Kim, D., Kim, Y.H., Kwon, S., 2018. Enhanced nasal drug delivery efficiency by increasing mechanical loading using hypergravity. Sci. Rep. 8, 168.
Kippax, P., Krarup, H., Suman, J.D., 2004. Application for Droplet Sizing: Manual Versus Automated Actuation of Nasal Sprays, 28.
Kippax, P., Fracassi, J., 2003. Particle Size Characterisation in Nasal Sprays and Aerosols. LabPlus Int.
Kreft, M.E., et al., 2015. The characterization of the human nasal epithelial cell line RPMI 2650 under different culture conditions and their optimization for an appropriate in vitro nasal model. Pharm. Res. 32, 665–679.
Kulkarni, A.D., Bari, D.B., Surana, S.J., Pardeshi, C.V., 2016. In vitro, ex vivo and in vivo performance of chitosan-based spray-dried nasal mucoadhesive microspheres of diltiazem hydrochloride. J. Drug Deliv. Sci. Technol. 31, 108–117.
Kulkarni, V., Shaw, C., 2012. Formulation and characterization of nasal sprays. An examination of nasal spray formulation parameters and excipients and their influence on key in vitro tests. Inhalation 10–15.
Kumar, H., et al., 2018. Intranasal drug delivery: a non-invasive approach for the better delivery of neurotherapeutics. Pharm. Nanotechnol. 5.
Kumar, A., Pandey, A.N., Jain, S.K., 2014. Nasal-nanotechnology: revolution for efficient therapeutics delivery. Drug Deliv. 1–13. https://doi.org/10.3109/10717544.2014.920431.
Kundoor, V., Dalby, R.N., 2011. Effect of formulation- and administration-related variables on deposition pattern of nasal spray pumps evaluated using a nasal cast. Pharm. Res. 28, 1895–1904.
Le Guellec, S., et al., 2014. Validation of anatomical models to study aerosol deposition in human nasal cavities. Pharm. Res. 31, 228–237.
Lee, M.-K., et al., 2005. Air-liquid interface culture of serially passaged human nasal epithelial cell monolayer for in vitro drug transport studies. Drug Deliv. 12, 305–311.
Lee, M., et al., 2017. Sinonasal delivery of resveratrol via mucoadhesive nanostructured microparticles in a nasal polyp mouse model. Sci. Rep. 7, 40249.
Leung, Sau-Hung Spence, Robinson, J.R., 1987. The contribution of anionic polymer structural features to mucoadhesion. J. Control. Release 5, 223–231.
Li, L., et al., 2006. Carbopol-mediated paracellular transport enhancement in Calu-3 cell layers. J. Pharm. Sci. 95, 326–335.
Lin, T., et al., 2016. Nose-to-brain delivery of macromolecules mediated by cell-penetrating peptides. Acta Pharm. Sin. B 6, 352–358.
Lin, J.K., Wheatley, F.C., Handwerker, J., Harris, N.J., Wong, B.J.F., 2014. Analyzing nasal septal deviations to develop a new classification system: a computed tomography study using MATLAB and OsiriX. JAMA Facial Plast. Surg. 16, 183–187.
Lindemann, J., Leiacker, R., Rettinger, G., Keck, T., 2002. Nasal mucosal temperature during respiration. Clin. Otolaryngol. Allied Sci. 27, 135–139.
Liu, X., Doub, W.H., Guo, C., 2010. Evaluation of droplet velocity and size from nasal spray devices using phase Doppler anemometry (PDA). Int. J. Pharm. 388, 82–87.
Longenecker, J.P., et al., 1987. Effects of sodium taurodihydrofusidate on nasal absorption of insulin in sheep. J. Pharm. Sci. 76, 351–355.
Lungare, S., Bowen, J., Badhan, R., 2016. Development and evaluation of a novel intranasal spray for the delivery of amantadine. J. Pharm. Sci. 105, 1209–1220.
Luthringer, R., et al., 2009. Rapid absorption of sumatriptan powder and effects on glyceryl trinitrate model of headache following intranasal delivery using a novel bidirectional device. J. Pharm. Pharmacol. 61, 1219–1228.
Mahajan, H.S., Mahajan, M.S., Nerkar, P.P., Agrawal, A., 2014. Nanoemulsion-based intranasal drug delivery system of saquinavir mesylate for brain targeting. Drug Deliv. 21, 148–154.
Majima, Y., et al., 1999. Effect of Biochemical Components on Rheologic Properties of Nasal Mucus in Chronic Sinusitis. Am. J. Respir. Crit. Care Med. 160, 421–426.
Majima, Y., Hirata, K., Keuchi, K.T., Hattori, M., Sakakura, Y., 1990. Effects of orally administered drugs on dynamic viscoelasticity of human nasal mucus. Am. Rev. Respir. Dis. 141, 79–83.
Makidon, P.E., et al., 2010. Characterization of stability and nasal delivery systems for immunization with nanoemulsion-based vaccines. J. Aerosol Med. Pulm. Drug Deliv. 23, 77–89.
Mantle, M., Allen, A., 1978. A colorimetric assay for glycoproteins based on the periodic acid/Schiff stain [proceedings]. Biochem. Soc. Trans. 6, 607–609.
Martignoni, I., et al., 2016. Resveratrol solid lipid microparticles as dry powder formulation for nasal delivery, characterization and in vitro deposition study. J. Microencapsul. 33, 735–742.
Marx, D., Birkhoff, M., 2011. Multi-dose container for nasal and ophthalmic drugs: a preservative free future? Drug Development – A Case Study Based Insight into Modern Strategies. InTech doi: 10.5772/27767.
Masiuk, T., Kadakia, P., Wang, Z., 2016. Development of a physiologically relevant dripping analytical method using simulated nasal mucus for nasal spray formulation analysis. J. Pharm. Anal. 6, 283–291.
Mathias, N.R., et al., 2002. Permeability characteristics of Calu-3 human bronchial epithelial cells: in vitro – in vivo correlation to predict lung absorption in rats. J. Drug Target 10, 31–40.
McMartin, C., Hutchinson, L.E., Hyde, R., Peters, G.E., 1987. Analysis of structural requirements for the absorption of drugs and macromolecules from the nasal cavity. J. Pharm. Sci. 76, 535–540.
Meeting at Washington. United States Pharmacopoeia, National Formulary. By authority of united state Pharmacopoeia Convention, Inc., 2004.
Meindl, C., et al., 2015. Permeation of therapeutic drugs in different formulations across the airway epithelium in vitro. PLoS One 10, e0135690.
Menzel, C., Jelkmann, M., Laffleur, F., Bernkop-Schnürch, A., 2017. Nasal drug delivery: design of a novel mucoadhesive and in situ gelling polymer. Int. J. Pharm. 517, 196–202.
Merkus, Verhoef, Schipper, Marttin, 1998. Nasal mucociliary clearance as a factor in nasal drug delivery. Adv. Drug Deliv. Rev. 29, 13–38.
Minne, A., Boireau, H., Horta, M.J., Vanbever, R., 2008. Optimization of the aerosolization properties of an inhalation dry powder based on selection of excipients. Eur. J. Pharm. Biopharm. 70, 839–844.
Mitchell, J.P., Nagel, M.W., Nichols, S., Nerbrink, O., 2006. Laser diffractometry as a technique for the rapid assessment of aerosol particle size from inhalers. J. Aerosol Med. 19, 409–433.
Moore, G.E., Sandberg, A.A., 1964. Studies of a human tumor cell line with a diploid karyotype. Cancer 17, 170–175.
Moraga-Espinoza, D., Warnken, Z., Moore, A., Williams, R.O., Smyth, H.D.C., 2018. A modified USP induction port to characterize nasal spray plume geometry and predict turbinate deposition under flow. Int. J. Pharm. 548, 305–313.
Moulton, D.G., 1971. The Olfactory Pigment. Springer, Berlin, Heidelberg, pp. 59–74 doi: 10.1007/978-3-642-65126-7_3.
Nagda, C.D., Chotai, N.P., Nagda, D.C., Patel, S.B., Patel, U.L., 2011. Development and characterization of mucoadhesive microspheres for nasal delivery of ketorolac. Pharmazie 66, 249–257.
Naik, A., Nair, H., 2014. Formulation and evaluation of thermosensitive biogels for nose to brain delivery of doxepin. Biome 2014.
Nakamura, F., Ohta, R., Machida, Y., Nagai, T., 1996. In vitro and in vivo nasal mucoadhesion of some water-soluble polymers. Int. J. Pharm. 134, 173–181.
Nemichand, S.K., Laxman, S.D., 2016. Solubility enhancement of nebivolol by micro emulsion technique. J. Young Pharm. 8, 356–367.
Ng, S.-F., Rouse, J.J., Sanderson, F.D., Meidan, V., Eccleston, G.M., 2010. Validation of a static Franz diffusion cell system for in vitro permeation studies. AAPS PharmSciTech 11, 1432–1441.
Niazi, S.K., 2004. Handbook of Pharmaceutical Manufacturing Formulations: Liquid Products (Volume 3 of 6). CRC Press.
Niazi, S., 2015. Handbook of Bioequivalence Testing. CRC Press.
Nicolazzo, J.A., Reed, B.L., Finnin, B.C., 2003. The effect of various in vitro conditions on the permeability characteristics of the buccal mucosa. J. Pharm. Sci. 92, 2399–2410.
Nolte, M., et al., 1990. Biological activity of nasally administered insulin in normal subjects. Horm. Metab. Res. 22, 170–174.
Ohashi, Y., et al., 1988. Toxicity of isopropyl alcohol exposure on the nasal mucociliary system in the guinea pig. Environ. Res. 46, 25–38.
Ong, H.X., et al., 2016. Primary air-liquid interface culture of nasal epithelium for nasal drug delivery. Mol. Pharm. 13, 2242–2252.
Ozsoy, Y., Gungor, S., Cevher, E., 2009. Nasal delivery of high molecular weight drugs. Molecules 14, 3754–3779.

Pandey, P., Cabot, P.J., Wallwork, B., Panizza, B.J., Parekh, H.S., 2017. Formulation, functional evaluation and ex vivo performance of thermoresponsive soluble gels – a platform for therapeutic delivery to mucosal sinus tissue. Eur. J. Pharm. Sci. 96, 499–507.
Pardeshi, V., Belgamwar, V.S., 2013. Direct nose to brain drug delivery via integrated nerves pathway bypassing the blood brain barrier:an excellent pathway for brain targetting. Exper. Opin. Drug Deliv. 10, 957–972.
Park, D.Y., Kim, S., Kim, C.H., Yoon, J.H., Kim, H.J., 2016. Alternative method for primary nasal epithelial cell culture using intranasal brushing and feasibility for the study of epithelial functions in allergic rhinitis. Allergy. Asthma Immunol. Res. 8, 69–78.
Passali, D., Bellussi, L., Lauriello, M., Passali, D., 1995. The rheological characteristics of nasal mucus in patients with rhinitis. Eur. Arch. Oto-Rhino-Laryngology 252.
Patel, R., Patel, M., Kashyap, B., Patel, G.B., 2013. Formulation consideration and characterization of microemulsion drug delivery system for transnasal administration of carbamazepine. Bull. Fac. Pharmacy, Cairo Univ. 51.
Pathak, K., 2011. Mucoadhesion; a prerequisite or a constraint in nasal drug delivery? Int. J. Pharm. Investig. 1, 62–63.
Pathak, Y., Thassu, D. Drug Delivery Nanoparticles Formulation and Characterization, 2009.
Pathak, R., Prasad Dash, R., Misra, M., Nivsarkar, M., 2014. Role of mucoadhesive polymers in enhancing delivery of nimodipine microemulsion to brain via intranasal route. Acta Pharm. Sin. B 4, 151–160.
Patil, S., Murthy, R., 2006. Preparation and in vitro evaluation of mucoadhesive chitosan microspheres of amlodipine besylate for nasal administration. Indian J. Pharm. Sci. 68, 64.
Patil, S., Babbar, A., Mathur, R., Mishra, A., Sawant, K., 2010. Mucoadhesive chitosan microspheres of carvedilol for nasal administration. J. Drug Target. 18, 321–331.
Pavanetto, F., Genta, I., Giunchedi, P., Conti, B., Conte, U., 1994. Spray-dried albumin microspheres for the intra-articular delivery of dexamethasone. J. Microencapsul. 11, 445–454.
Pavis, H., et al., 2002. Pilot study of nasal morphine-chitosan for the relief of breakthrough pain in patients with cancer. J. Pain Symptom Manage. 24, 598–602.
Pawar, D., et al., 2010. Evaluation of mucoadhesive PLGA microparticles for nasal immunization. AAPS J. 12, 130–137.
Pawar, D., Jaganathan, K.S., 2016. Mucoadhesive glycol chitosan nanoparticles for intranasal delivery of hepatitis B vaccine: enhancement of mucosal and systemic immune response. Drug Deliv. 23, 185–194.
Pennington, J., Pandey, P., Tat, H., Willson, J., Donovan, B., 2008. Spray pattern and droplet size analyses for high-shear viscosity determination of aqueous suspension corticosteroid nasal sprays. Drug Dev. Ind. Pharm. 34, 923–929.
Pires, A., Fortuna, A., Alves, G., Falcão, A., 2009. Intranasal drug delivery: how, why and what for? J. Pharm. Pharm. Sci. 12, 288–311.
Ponec, M., 1992. In vitro cultured human skin cells as alternatives to animals for skin irritancy screening. Int. J. Cosmet. Sci. 14, 245–264.
Pozzoli, M., et al., 2016b. Application of RPMI 2650 nasal cell model to a 3D printed apparatus for the testing of drug deposition and permeation of nasal products. Eur. J. Pharm. Biopharm. 107, 223–233.
Pozzoli, M., et al., 2016a. Dry powder nasal drug delivery: challenges, opportunities and a study of the commercial Teijin Puvlizer Rhinocort device and formulation. Drug Dev. Ind. Pharm. 42, 1660–1668.
Pozzoli, M. et al., 2014. Optimization of RPMI 2650 Cells as a Model for Nasal Mucosa.
Pozzoli, M., 2017. Drug delivery to the nose : formulation, deposition and permeation of poorly soluble drugs.
Pu, Y., Goodey, A.P., Fang, X., Jacob, K., 2014. A comparison of the deposition patterns of different nasal spray formulations using a nasal cast. Aerosol Sci. Technol. 48, 930–938.
Pund, S., Rasve, G., Borade, G., 2013. Ex vivo permeation characteristics of venlafaxine through sheep nasal mucosa. Eur. J. Pharm. Sci. 48, 195–201.
Rao, K.V.R., Buri, P., 1989. A novel in situ method to test polymers and coated microparticles for bioadhesion. Int. J. Pharm. 52, 265–270.
Reichl, S., Becker, K., 2012. Cultivation of RPMI 2650 cells as an in-vitro model for human transmucosal nasal drug absorption studies: optimization of selected culture conditions. J. Pharm. Pharmacol. 64, 1621–1630.
Ren, D., Daines, D.A., 2011. Use of the EpiAirway model for characterizing long-term host-pathogen interactions. J. Vis. Exp. https://doi.org/10.3791/3261. e3261.
Rhee, C.-S., et al., 1999. Effects of mucokinetic drugs on rheological properties of reconstituted human nasal mucus. Arch. Otolaryngol. Neck Surg. 125, 101.
Rochat, T., Lacroix, J.-S., Jornot, L., 2004. N-acetylcysteine inhibits Na+ absorption across human nasal epithelial cells. J. Cell. Physiol. 201, 106–116.
Röhm, M., et al., 2017. A comprehensive screening platform for aerosolizable protein formulations for intranasal and pulmonary drug delivery. Int. J. Pharm. 532, 537–546.
Salade, L., et al., 2017. Development of coated liposomes loaded with ghrelin for nose-to-brain delivery for the treatment of cachexia. Int. J. Nanomedicine 12, 8531–8543.
Salade, L., Wauthoz, N., Vermeersch, M., Amighi, K., Goole, J., 2018. Chitosan-coated liposome dry-powder formulations loaded with ghrelin for nose-to-brain delivery. Eur. J. Pharm. Biopharm. 129, 257–266.
Sangolkar, S., Adhao, V., Mundhe, D., Sawarkar, H., 2012. Particle size determination of nasal drug delivery system: a review. Int. J. Pharm. Sci. Rev. Res. 17, 66–73.
Scherließ, R., 2010. Comparison of in vitro methods to determine nasal versus lung deposition of a protein formulation.
Scherließ, R., Trows, S., 2011. Novel formulation concept for particulate uptake of vaccines via the nasal associated lymphoid tissue. Procedia Vaccinol. 4, 113–119.
Schipper, N.G.M., Verhoef, J.C., Merkus, F.W.H.M., 1991. The nasal mucociliary clearance: relevance to nasal drug delivery. Pharm. Res. 8, 807–814.
Schmidt, M.C., et al., 2000. Validation of excised bovine nasal mucosa as in vitro model to study drug transport and metabolic pathways in nasal epithelium. J. Pharm. Sci. 89, 396–407.
Schmidt, M.C., Peter, H., Lang, S.R., Ditzinger, G., Merkle, H.P., 1998. In vitro cell models to study nasal mucosal permeability and metabolism. Adv. Drug Deliv. Rev. 29, 51–79.
Schögler, A., et al., 2017. Characterization of pediatric cystic fibrosis airway epithelial cell cultures at the air-liquid interface obtained by non-invasive nasal cytology brush sampling. Respir. Res. 18, 215.
Schroeter, J.D., Tewksbury, E.W., Wong, B.A., Kimbell, J.S., 2015. Experimental measurements and computational predictions of regional particle deposition in a sectional nasal model. J. Aerosol Med. Pulm. Drug Deliv. 28, 20–29.
Sekerdag, E., 2017. Challenges of the nose-to-brain route. In: Nanotechnology Methods for Neurological Diseases and Brain Tumors. Elsevier, pp. 103–113 doi: 10.1016/B978-0-12-803796-6.00006-X.
Seki, T., Kanbayashi, H., Chono, S., Tabata, Y., Morimoto, K., 2007. Effects of a sperminated gelatin on the nasal absorption of insulin. Int. J. Pharm. 338, 213–218.
Shah, S.A., et al., 2014. Design of experiments to optimize an in vitro cast to predict human nasal drug deposition. J. Aerosol Med. Pulm. Drug Deliv. 27, 21–29.
Shah, B., Khunt, D., Misra, M., Padh, H., 2016. Non-invasive intranasal delivery of quetiapine fumarate loaded microemulsion for brain targeting: formulation, physicochemical and pharmacokinetic consideration. Eur. J. Pharm. Sci. 91, 196–207.
Shah, B.M., Misra, M., Shishoo, C.J., Padh, H., 2015. Nose to brain microemulsion-based drug delivery system of rivastigmine: formulation and ex-vivo characterization. Drug Deliv. 22, 918–930.
Shargel, L., Kanfer, I., 2010. Generic Drug Product Development: Specialty Drug Forms. Informa Healthcare.
Shaw, C.L., Dymock, R.B., Cowin, A., Wormald, P.J., 2000. Effect of packing on nasal mucosa of sheep. J. Laryngol. Otol. 114, 506–509.
Shen, B.Q., Finkbeiner, W.E., Wine, J.J., Mrsny, R.J., Widdicombe, J.H., 1994. Calu-3: a human airway epithelial cell line that shows cAMP-dependent Cl- secretion. Am. J. Physiol. 266, L493–L501.
Shi, H., Kleinstreuer, C., Zhang, Z., 2007. Modeling of inertial particle transport and deposition in human nasal cavities with wall roughness. J. Aerosol Sci. 38, 398–419.
Shin, B.S., Jung, J.H., Lee, K.C., Yoo, S.D., 2004. Nasal absorption and pharmacokinetic disposition of salmon calcitonin modified with low molecular weight polyethylene glycol. Chem. Pharm. Bull. (Tokyo) 52, 957–960.
Shinichiro, H., Takatsuka, Y., Tai, M., Hiroyuki, M., 1981. Absorption of drugs from the nasal mucosa of rat. Int. J. Pharm. 7, 317–325.
Sigurdsson, H.H., Kirch, J., Lehr, C.-M., 2013. Mucus as a barrier to lipophilic drugs. Int. J. Pharm. 453, 56–64.
Sonvico, F., et al., 2018. Surface-modified nanocarriers for nose-to-brain delivery: from bioadhesion to targeting. Pharmaceutics 10, 34.
Spraytec Nasal Spray Support for accurate nasal spray droplet sizing from Malvern Instruments. Available at: https://www.malvernpanalytical.com/en/products/product-range/spraytec/accessories/nasal-spray-accessory. (Accessed: 19th September 2018).
Srinivasan, B., et al., 2015. TEER measurement techniques for in vitro barrier model systems. J. Lab. Autom. 20, 107–126.
Stanley, P.J., Wilson, R., Greenstone, M.A., Macwilliam, L., Cole, P.J., 1986. Effect of cigarette smoking on nasal mucociliary clearance and ciliary beat frequency. Thorax 41.
Stoker, D.G., et al., 2008. Analgesic efficacy and safety of morphine-chitosan nasal solution in patients with moderate to severe pain following orthopedic surgery. Pain Med. 9, 3–12.
Subramaniam, R.P., Richardson, R.B., Morgan, K.T., Kimbell, J.S., Guilmette, R.A., 1998. Computational fluid dynamics simulations of inspiratory airflow in the human nose and nasopharynx. Inhal. Toxicol. 10, 91–120.
Suman, J.D., Laube, B.L., Dalby, R., 1999. Comparison of nasal deposition and clearance of aerosol generated by nebulizer and an aqueous spray pump. Pharm. Res. 16, 1648–1652.
Suman, J.D., Laube, B.L., Lin, T.-C., Brouet, G., Dalby, R., 2002. Validity of in vitro tests on aqueous spray pumps as surrogates for nasal deposition. Pharm. Res. 19, 1–6.
Swamy, N.G.N., Abbas, Z., 2011. Preparation and in vitro characterization of mucoadhesive hydroxypropyl guar microspheres containing amlodipine besylate for nasal administration. Indian J. Pharm. Sci. 73, 608–614.
Takeuchi, H., Yamamoto, H., Niwa, T., Hino, T., Kawashima, Y., 1996. Enteral absorption of insulin in rats from mucoadhesive chitosan-coated liposomes. Pharm. Res. 13, 896–901.
Tas, C., et al., 2009. Nasal administration of metoclopramide from different dosage forms: in vitro, ex vivo, and in vivo evaluation. Drug Deliv. 16, 167–175.
Terauchi, Y., et al., 2018. IgA polymerization contributes to efficient virus neutralization on human upper respiratory mucosa after intranasal inactivated influenza vaccine administration. Hum. Vaccin. Immunother. 00–00. https://doi.org/10.1080/21645515.2018.1438791.
Thomas, R.J., Hacking, A., Brooks, T.J.G., 2007. Structural modification of a base disaccharide alters antiadhesion properties towards Yersinia pestis. FEMS Immunol. Med. Microbiol. 49, 410–414.
Tiozzo Fasiolo, L., et al., 2018. Opportunity and challenges of nasal powders: drug formulation and delivery. Eur. J. Pharm. Sci. 113, 2–17.
Trows, S., Wuchner, K., Spycher, R., Steckel, H., 2014. Analytical challenges and regulatory requirements for nasal drug products in Europe and the U.S. Pharmaceutics 6, 195–219.
Türker, S., Onur, E., Özer, Y., 2004. Nasal route and drug delivery systems. Pharm. World Sci. 26, 137–142.
Ulm, A., Mayhew, C.N., Debley, J., Khurana Hershey, G.K., Ji, H., 2016. Cultivate primary

nasal epithelial cells from children and reprogram into induced pluripotent stem cells. J. Vis. Exp. https://doi.org/10.3791/53814.
Ument Karasulu, E., et al., 2008. Permeation studies and histological examination of sheep nasal mucosa following administration of different nasal formulations with or without absorption enhancers. Drug Deliv. 15, 219–225.
Upadhyay, P., Trivedi, J., Pundarikakshudu, K., Sheth, N., 2017. Direct and enhanced delivery of nanoliposomes of anti schizophrenic agent to the brain through nasal route. Saudi Pharm. J. 25, 346–358.
Van der Walle, C., 2011. Peptide and Protein Delivery. Academic Press.
van Woensel, M., et al., 2013. Formulations for intranasal delivery of pharmacological agents to combat brain disease: a new opportunity to tackle GBM? Cancers (Basel). 5, 1020–1048.
Varshosaz, J., Sadrai, H., Heidari, A., 2006. Nasal delivery of insulin using bioadhesive chitosan gels. Drug Deliv. 13, 31–38.
Vasa, D.M., Buckner, I.S., Cavanaugh, J.E., Wildfong, P.L.D., 2017. Improved flux of levodopa via direct deposition of solid microparticles on nasal tissue. AAPS PharmSciTech 18, 904–912.
Viegas, D.A., et al., 2016. Development and application of an ex vivo fosphenytoin nasal bioconversion/permeability evaluation method. PHASCI 89, 61–72.
Wan, H., et al., 2000. Tight junction properties of the immortalized human bronchial epithelial cell lines Calu-3 and 16HBE14o-. Eur. Respir. J. 15, 1058–1068.
Wang, Y., et al., 2016. Zolpidem mucoadhesive formulations for intranasal delivery: characterization, in vitro permeability, pharmacokinetics, and nasal ciliotoxicity in rats. J. Pharm. Sci. 105, 2840–2847.
Wang, Y., Jiang, S., Wang, H., Bie, H., 2017. A mucoadhesive, thermoreversible in situ nasal gel of geniposide for neurodegenerative diseases. PLoS One 12, e0189478.
Wen, M.M., 2011. Olfactory targeting through intranasal delivery of biopharmaceutical drugs to the brain: current development. Discov. Med. 11, 497–503.
Wengst, A., Reichl, S., 2009. RPMI 2650 epithelial model and three-dimensional reconstructed human nasal mucosa as in vitro models for nasal permeation studies. Eur. J. Pharm. Biopharm. 74, 290–297.
Williams, G., Blatchford, C., Mitchell, J.P., 2018. Evaluation of nasal inlet ports having simplified geometry for the pharmacopeial assessment of mass fraction of dose likely to penetrate beyond the nasopharynx: a preliminary investigation. AAPS PharmSciTech 19, 3723–3733.
Wilson, W.R., Allansmith, M.R., 1976. Rapid, Atraumatic method for obtaining nasal mucus samples. Ann. Otol. Rhinol. Laryngol. 85, 391–393.
Witschi, C., Mrsny, R.J., 1999. In vitro evaluation of microparticles and polymer gels for use as nasal platforms for protein delivery. Pharm. Res. 16, 382–390.
Wu, R., Yankaskas, J., Cheng, E., Knowles, M.R., Boucher, R., 1985. Growth and differentiation of human nasal epithelial cells in culture. Serum-free, hormone-supplemented medium and proteoglycan synthesis. Am. Rev. Respir. Dis. 132, 311–320.
Xi, J., et al., 2016a. Visualization and quantification of nasal and olfactory deposition in a sectional adult nasal airway cast. Pharm. Res. An Off. J. Am. Assoc. Pharm. Sci. Pharm Res 33, 1527–1541.
Xi, J., Kim, J., Si, X.A., Corley, R.A., Zhou, Y., 2016b. Modeling of inertial deposition in scaled models of rat and human nasal airways: towards in vitro regional dosimetry in small animals. J. Aerosol Sci. 99, 78–93.
Xi, J., Si, X.A., 2017. Numerical simulation and experimental testing to improve olfactory drug delivery with electric field guidance of charged particles. In: Advanced Technology for Delivering Therapeutics. InTech. https://doi.org/10.5772/65858.
Xie, Y., et al., 2006. Preparation of bupleurum nasal spray and evaluation on its safety and efficacy. Chem. Pharm. Bull. (Tokyo) 54, 48–53.
Yarragudi, S.B., et al., 2017. Formulation of olfactory-targeted microparticles with tamarind seed polysaccharide to improve nose-to-brain transport of drugs. Carbohydr. Polym. 163, 216–226.
Ye, Y., et al., 2013. DNA-loaded chitosan oligosaccharide nanoparticles with enhanced permeability across Calu-3 cells. J. Drug Target. 21, 474–486.
Yoo, J.-W., et al., 2003. Serially passaged human nasal epithelial cell monolayer for in vitro drug transport studies. Pharm. Res. 20, 1690–1696.
Yu, T., Andrews, G.P., Jones, D.S., 2014. Mucoadhesion and characterization of mucoadhesive properties. In: Mucosal Delivery of Biopharmaceuticals. Springer, US, pp. 35–58 doi: 10.1007/978-1-4614-9524-6_2.
Yu, G., Zhang, Z., Lessmann, R., 1998. Fluid Flow and Particle Diffusion in the Human Upper Respiratory System. Aerosol Sci. Technol. 28, 146–158.
Zhang, Y., et al., 2005. Permeation-enhancing effects of chitosan formulations on recombinant hirudin-2 by nasal delivery in vitro and in vivo. Acta Pharmacol. Sin. 26, 1402–1408.
Zhang, L., et al., 2016. Puerarin transport across a Calu-3 cell monolayer – an in vitro model of nasal mucosa permeability and the influence of paeoniflorin and menthol. Drug Des. Devel. Ther. 10, 2227–2237.